Microbiology and Infectious Disease

RNA polymerase III is involved in regulating *Plasmodium falciparum* virulence

Reviewed Preprint

Revised by authors after peer review.

About eLife's process

Reviewed preprint version 2
April 11, 2024 (this version)

Reviewed preprint version 1
February 28, 2024

Posted to preprint server
January 15, 2024

Sent for peer review
January 12, 2024

Gretchen Diffendall, Aurélie Claës, Anna Barcons-Simon, Prince Nyarko, Florent Dingli, Miguel Santos, Damarys Loew, Antoine Claessens, Artur Scherf

Institut Pasteur, 1Universite Paris Cité, INSERM U1201, CNRS EMR9195, Paris, France • Sorbonne Université Ecole doctorale Complexité du Vivant ED515, Paris, France • Biomedical Center, Division of Physiological Chemistry, Faculty of Medicine, Ludwig-Maximilians- Universität München, Munich 82152, Germany • Laboratory of Pathogen–Host Interaction (LPHI), CNRS, University of Montpellier, France • Institut Curie, PSL Research University, Centre de Recherche, CurieCoreTech Mass Spectrometry Proteomics, Paris, France • Instituto de Medicina Molecular João Lobo Antunes, Faculdade de Medicina da Universidade de Lisboa, Lisboa, Portugal • LPHI, MIVEGEC, CNRS, INSERM, University of Montpellier, France

Abstract

While often undetected and untreated, persistent seasonal asymptomatic malaria infections remain a global public health problem. Despite the presence of parasites in the peripheral blood, no symptoms develop. Disease severity is correlated with the levels of infected red blood cells (iRBCs) adhering within blood vessels. Changes in iRBC adhesion capacity have been linked to seasonal asymptomatic malaria infections, however how this is occurring is still unknown. Here we present evidence that RNA polymerase III (RNA Pol III) transcription in *Plasmodium falciparum* is downregulated in field isolates obtained from asymptomatic individuals during the dry season. Through experiments with in vitro cultured parasites, we have uncovered an RNA Pol III-dependent mechanism that controls pathogen proliferation and expression of a major virulence factor in response to external stimuli. Our findings establish a connection between *P. falciparum* cytoadhesion and a non-coding RNA family transcribed by Pol III. Additionally, we have identified *P. falciparum* Maf1 as a pivotal regulator of Pol III transcription, both for maintaining cellular homeostasis and responding adaptively to external signals. These results introduce a novel perspective that contributes to our understanding of *P. falciparum* virulence. Furthermore, they establish a connection between this regulatory process and the occurrence of seasonal asymptomatic malaria infections.

eLife assessment

This **important** study links the activity of polymerase III to the regulation of virulence gene expression in the deadliest malaria parasite, Plasmodium falciparum. It identifies Maf1 as a Pol III inhibitor that enables the parasite to respond to external stimuli such as magnesium chloride plasma levels by downregulating Pol III-transcribed ruf6 genes and subsequently regulated var genes. While the evidence presented is generally **convincing**, some of the results are **incomplete**, and the mechanistic link between external signals and Maf1 activation remains unknown.

Introduction

The parasite *Plasmodium falciparum* is responsible for the deadliest form of human malaria that annually affects over 200 million people, with 619,000 fatal cases, majorly African children under the age of 5. The disease is transmitted to its human host during a blood meal by the parasites' vector, *Anopheles* mosquitoes. Disease symptoms are seen while the parasite multiplies asexually within the host RBCs. During this time, variant surface antigens (VSAs) are exported and displayed on the surface of the iRBCs (Wahlgren *et al*, 2017). During the ~48-hour asexual intraerythrocytic developmental cycle (IDC), the parasite develops through different morphological stages: ring (circulating), trophozoite, and schizont (sequestered in capillaries). Expression of one type of VSA that is linked to immune evasion and pathogenesis, termed *P. falciparum* erythrocyte membrane protein 1 (PfEMP1) (Leech *et al*, 1984), can bind to a wide range of receptors on endothelial cells such as CD36. PfEMP1 binding mediates adhesion to the vascular endothelium within the host, thereby preventing mature iRBCs from traveling to, and being cleared by, the spleen (Smith *et al*, 2013). *Plasmodium* parasites replicate via schizogony inside the host RBCs generating the infectious form, termed merozoites. Upon bursting of the iRBC, merozoites invade new RBCs, thus enabling the cycle to restart. The number of merozoites per schizont has been shown to reduce in unfavorable conditions as a way to diminish the total parasite load and therefore overall disease severity (Mancio-Silva *et al*, 2017b).

1. *P. falciparum* chronic infection relies largely on mutually exclusive expression of PfEMP1 surface adhesins, that are encoded by the *var* virulence gene family (Scherf *et al*, 1998; Smith *et al*, 1995; Guizetti & Scherf, 2013). The expression of *var* genes, while under tight epigenetic regulation by the parasite, is additionally controlled by a family of ncRNA, termed RUF6. *P. falciparum* 3D7 encodes 15 RUF6 genes dispersed over several chromosomes located adjacent to central *var* genes (Gardner *et al*, 2002). RUF6 ncRNA have been observed to associate with the active *var* gene in *trans* and transcriptional repression disrupts the monoallelic expression of *var* genes by down-regulating the entire *var* gene family (Barcons- Simon *et al*, 2020; Guizetti *et al*, 2016). Genetically modified parasites that express the entire RUF6 gene family show a general upregulation of *var* genes (Zhang *et al*, 2014; Fan *et al*, 2020).

2. *P.* falciparum virulence is linked to cytoadhesion and sequestration as a result of reduced clearance of iRBCs in the spleen and increased microcapillary obstruction and local inflammation (Miller *et al*, 2002). Substantial sequestration of iRBCs in critical target organs has been associated with severe malaria (Miller *et al*, 2013; Guillochon *et al*, 2022). In long- term asymptomatic infections, found during prolonged low transmission dry seasons in malaria-endemic regions, decreased cytoadhesion and longer circulation time of iRBCs in the blood has been observed (Andrade *et al*, 2020). It is not fully understood how asymptomatic infections develop and are maintained nor is a molecular understanding of host and parasite factors, that underlies disease severity during the dry and wet seasons (reviewed in (Zhang & Deitsch, 2022)). Disease severity appears to be influenced by a variety of factors derived from the human host, parasite, and environment. *Plasmodium* parasites are auxotrophic for various nutrients including glucose, certain types of amino acids, and lipids, which must be obtained from the host. Physiological conditions in the host, like diabetes, pregnancy, diet, and immunity can change the metabolic environment the parasites are exposed to. Numerous studies conclude that host immunity is a contributing factor to the maintenance of asymptomatic infections (Kimenyi *et al*, 2019). While it is proposed that *P. falciparum* virulence regulation contributes to decreased endothelial binding, the mechanism and factors involved remains to be determined.

Almost all eukaryotes use conserved nutrient sensing pathways, including mTOR, GCN2, GCN5, Rgt2/Snf3, and Snf1/AMPK signaling cascades (reviewed in (Kumar *et al*, 2021)). Most notably, the target of rapamycin complex (TORC) pathway involves the signaling of external factors to control many cellular processes (Wullschleger *et al*, 2006). Specifically, TORC participates in the regulation of RNA Pol III activity via the phosphorylation of its inhibitor, Maf1. When nutrients are available and mTOR kinase is active, Maf1 is hyperphosphorylated resulting in an inactive cytoplasmic state. Stress-induced Maf1 dephosphorylation results in nuclear localization and inhibition of RNA Pol III (Pluta *et al*, 2001; Rollins *et al*, 2007; Vannini *et al*, 2010). This pathway responds to a range of positive and negative external stimuli, most notably the presence of amino acids, that drive or inhibit cellular growth. The majority of the TORC pathway components are lost in the apicomplexan lineage (McLean & Jacobs-Lorena, 2017; Serfontein *et al*, 2010; van Dam *et al*, 2011). While *P. falciparum* encodes none of the core TORC1 components, it does contain a homologue to Maf1 (McLean & Jacobs-Lorena, 2017). The biology of *P. falciparum* Pf-Maf1 is still poorly characterized.

Here, we present data showing inhibition of RNA Pol III transcription in field isolates from asymptomatic individuals during the dry season. We present evidence for *P. falciparum* Maf1 as a negative regulator of RNA Pol III-transcribed genes including tRNA and RUF6 ncRNA, and demonstrate that this mechanism is responsive to external stimuli using *in vitro* culture. Inhibition of *P. falciparum* cytoadherence, via the regulation of RNA Pol III activity, represents a new paradigm contributing to *P. falciparum* virulence and links this process to seasonal asymptomatic malaria infections.

Results

RUF6 ncRNA is downregulated in asymptomatic individuals during the dry season

We and others have previously established the role of the 15-member RUF6 ncRNA gene family in *P. falciparum var* gene expression (Barcons-Simon *et al*, 2020; Diffendall *et al*, 2022; Fan *et al*, 2020; Guizetti *et al*, 2016). RUF6 ncRNA protein complex associates with the active *var* gene expression site (Diffendall *et al*, 2022; Guizetti *et al*, 2016), and knockdown of the ncRNA RUF6 gene family dramatically reduced *var* gene transcription (Barcons-Simon *et al*, 2020).

Bioinformatic analysis identified highly conserved RNA Pol III binding elements (conserved A- and B-box sequence) within RUF6 genes (Guizetti *et al*, 2016) (**Figure S1A**), hinting at a role for RNA Pol III in virulence gene regulation. Thus, we determined the effects of RNA Pol III inhibition on gene transcription in synchronized wild type parasites. We observed downregulation of tRNA and RUF6 transcription after 21 hours of treatment with a commercially available RNA Pol III inhibitor (**Figure S1B**). As expected, no changes were observed in the transcription of an RNA Pol II-regulated gene, *uce* (ubiquitin-conjugating enzyme, PF3D7_0812600) (**Figure S1B**). As predicted from the RUF6 sequence, our data provide direct experimental evidence for RNA Pol III-dependent transcription of RUF6 genes.

We next wanted to determine if RNA Pol III-transcribed genes, specifically RUF6 ncRNA, varied between parasites causing different clinical states of malaria infection, since previous studies did not include RNA Pol III-transcribed genes for their data analysis (Andrade *et al*, 2020). We first re-analyzed raw RNA-seq data, from a previous study that compared parasites infecting individuals during the dry versus wet season in a malaria endemic region of Mali (Andrade *et al*, 2020), to include these genes. We were able to retrieve transcriptional data for two RNA Pol III-transcribed tRNAs (tRNA Leucine Pf3D7_API05400 and tRNA Asparagine Pf3D7_API05500, **Figure S2A**), both of which show significantly lower levels in parasites infecting asymptomatic individuals during the dry season (n = 12) when compared to parasites infecting symptomatic individuals during the wet season (n = 12).

We further investigated whether RNA Pol III modulates gene transcription in field isolates of *P. falciparum* from different individuals infected during the wet and dry season in malaria endemic regions (The Gambia). In this pilot study, we analyzed *P. falciparum* steady state levels of RNA in venous blood samples taken from individuals with asymptomatic parasitemia during the dry season (n = 17), as well as mildly symptomatic malaria infections during the wet season (n = 14) in The Gambia (Collins *et al*, 2022; Fogang *et al*, 2023). RT- qPCR of total RNA showed that levels of tRNAs (Asparagine and Valine) were significantly lower ($p < 0.05$) in parasites from asymptomatic infections during the dry season compared to parasites causing symptomatic infections during the wet season (**Figure 1A**, B). Likewise, RUF6 ncRNA was significantly downregulated ($p < 0.005$) in parasites from asymptomatic infections during the dry season when compared to symptomatic infections during the wet season (**Figure 1C**). Expression was normalized to a housekeeping gene encoding fructose bisphosphate aldolase (Pf3D7_1444800).

The same previous study, mentioned above, also showed that *var* gene transcription varied in parasites infecting individuals during the dry versus wet seasons (Andrade *et al*, 2020). We observed a significantly lower level of *var* gene transcription ($p < 0.005$) in parasites taken from asymptomatic individuals during the dry season compared to those taken from symptomatic individuals during the wet season (**Figure 1D**). The observed lower transcript levels of *var* genes may be a direct result of reduced RUF6 ncRNA levels. Taken together, our results reveal that levels of RNA Pol III-transcribed genes, particularly the regulatory RUF6 ncRNA, varies significantly between two different clinical states and seasons.

The environmental factor, magnesium, plays a regulatory role in genes transcribed by RNA Polymerase III

In studies of malaria infections, variations in metabolite levels were observed between symptomatic and asymptomatic cases across wet and dry seasons. However, the data did not pinpoint any particular factor that could be reliably linked to a specific condition of the disease (Andrade *et al*, 2020). Other clinical studies investigated the correlation between macro- and micro-mineral concentrations and disease severity. In one study, it was discovered that levels of serum $MgCl_2$ were lower in cases of more severe malaria infections (Innocent *et al*, 2013). We chose to analyze plasma samples from individuals participating in the same study as referenced in

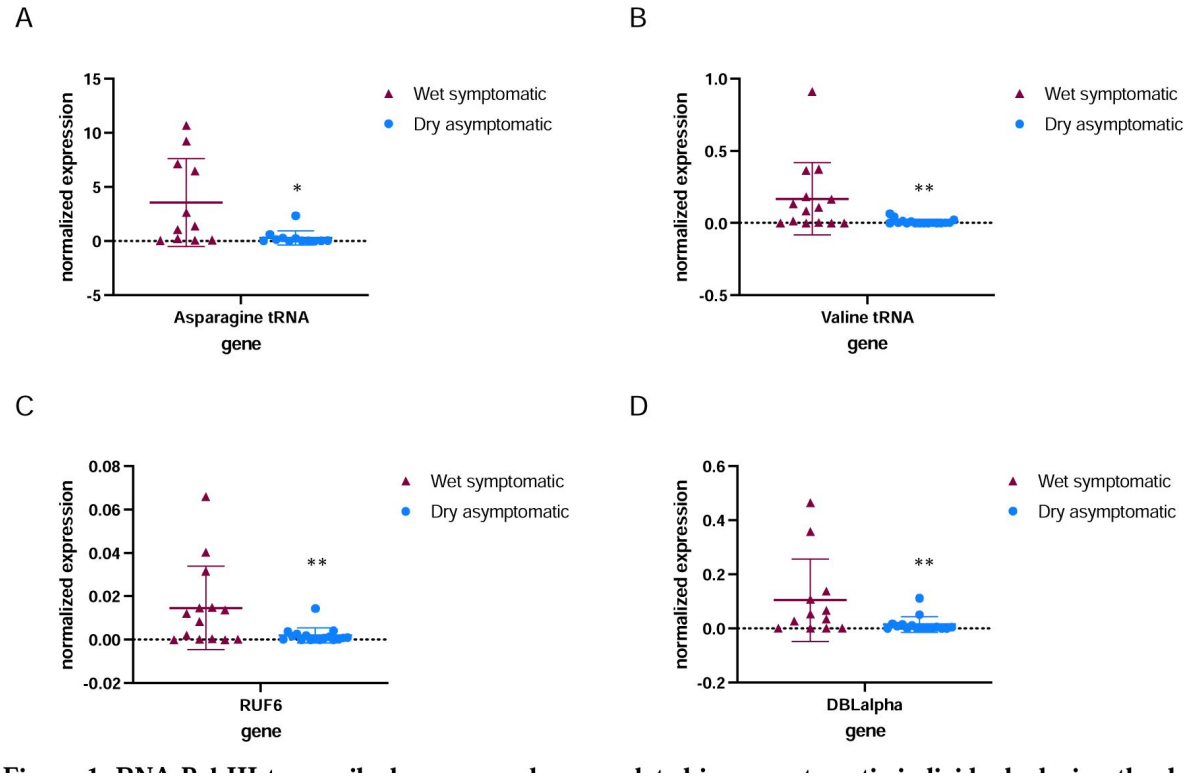

Figure 1.

RNA Pol III-transcribed genes are downregulated in asymptomatic individuals during the dry season.

Steady state RNA levels as quantified by RT-qPCR using primers to tRNA Asparagine (Pf3D7_0714700) (A) and tRNA Valine (Pf3D7_0312600) (B) as well as RNA Pol III-transcribed RUF6 ncRNA (C). DBLalpha primers were used to detect RNA Pol II-transcribed *var* genes (D). Normalized expression is shown using fructose-bisphosphate aldolase (FBA Pf3D7_1444800) as the reference gene in symptomatic individuals during the wet season (n = 14^{+}) and asymptomatic individuals during the dry season (n = 17^{+}). $^{+}$ with the exception of Asparagine tRNA wet symptomatic (n=11) and dry asymptomatic (n=12), and DBLalpha wet symptomatic (n = 12) and dry asymptomatic (n = 16). Box plots indicate the mean with standard deviation. Wilcoxon matched-pairs signed rank test was done to determine significance (* indicates $P < 0.05$ and ** indicates $P < 0.005$).

Figure 1, focusing on magnesium concentrations. Our findings show a significant increase in $MgCl_2$ levels in asymptomatic individuals during the dry season compared to symptomatic individuals in the wet season, as depicted in **Figure 2A**.

Our subsequent aim was to delve into the potential molecular mechanisms connecting external factors, like magnesium, with the changes in RUF6 ncRNA levels as shown in **Figure 2B**. For this, we employed in vitro cultured *P. falciparum* asexual blood stage parasites. We supplemented culture medium with $MgCl_2$, noted for its varying levels in individuals with malaria (see **Figure 2A**). In addition, we mimicked nutrient deprivation with isoleucine- deprived culture medium (as was described in (Babbitt *et al*, 2012; McLean & Jacobs-Lorena, 2017)), fever conditions with incubation at 40°C, and food starvation with low glucose levels (Jensen *et al*, 1983; Fang *et al*, 2004). We evaluated the steady state levels of RNA Pol I- (rRNA A1), RNA Pol II- (UCE and the active *var*), and RNA Pol III- (tRNA Valine and RUF6 ncRNA) transcribed genes in clonal parasites at late ring stage. We observed that high temperature and low glucose conditions affected gene transcription of RNA Pol I, II and Pol III (**Figure S2B**). Deprivation of isoleucine and $MgCl_2$ supplementation seemingly affected only RNA Pol III-transcribed genes with the exception of the RNA Pol II-transcribed active *var* gene, Pf3D7_1240900, likely as a result of decreased RUF6 ncRNA as was reported earlier (Barcons-Simon *et al*, 2020).

To explore the underlying molecular pathway that leads to the downregulation of RNA Pol III activity in malaria parasites, we continued using $MgCl_2$ supplementation. We selected a concentration of 3mM total $MgCl_2$, based on reports indicating it does not inhibit the growth of *P. falciparum* asexual blood stage and is within a physiological range (Jahnen-Dechent & Ketteler, 2012; Hess *et al*, 1995). Additionally, we verified lower magnesium concentrations and show as low as 1mM total $MgCl_2$, observed in healthy individuals, impacts both Pol III- transcribed RUF6 and tRNA, while not affecting Pol II-transcribed UCE (**Figure S3B**). RNA- seq was done on control and $MgCl_2$ supplemented cultured parasites during two time points of the asexual blood stage parasites (ring and trophozoite) to further confirm that RNA Pol III is the main target (**Figure 2C**, D). RNA-seq data was compared to the microarray time course data in (Bozdech *et al*, 2003) as in (Lemieux *et al*, 2009), which provided a statistical estimation of cell cycle progression at 12 and 24 hpi in both control and $MgCl_2$ supplemented parasites (**Figure S3B**).

These data indicate that any differences in transcription were due to $MgCl_2$ supplementation and not differences in cell cycle progression. During ring stage (**Figure 2C**), 77% of the down-regulated genes contain typical RNA Pol III promoter sequences, A- and B-box consensus (from **Figure S1A**). A total of 27 ncRNA genes were downregulated (logFC < 1.95, FDR < 0.05) including all 15 RUF6 ncRNA, 6 tRNAs, 1 spliceosomal RNA, and 4 snoRNA. Additionally, 12 protein coding genes were up-regulated with no conserved pathway nor molecular or biological process. During trophozoite stage (**Figure 2D**), 74% of the down- regulated genes have typical RNA Pol III promoter sequences. This demonstrates that $MgCl_2$ supplementation predominantly inhibits RNA Pol III-transcribed genes, including the entire RUF6 gene family.

Nuclear PfMaf1 protein is essential to regulate RNA Pol III

In almost all eukaryotes, the target of rapamycin complex (TORC) pathway has been shown to participate in the regulation of RNA Pol III activity via the phosphorylation of its only known inhibitor, Maf1 (**Figure 3A**, reviewed in (Wullschleger *et al*, 2006)). Upon phosphatase activation, modulated in response to external stimuli such as low nutrient availability, Maf1 shuttles to the nucleus to repress RNA Pol III activity (Michels *et al*, 2010). Because Maf1 is conserved in the apicomplexan lineage, a predicted essential blood stage protein in *P. falciparum*, we set out to explore if *P. falciparum* Maf1 (PfMaf1) functions similarly to model eukaryotes. We generated a PfMaf1 parasite line tagged with a 3HA tag and a ligand-controlled destabilization domain (ddFKBP), PfMaf1-FKBP (**Figure 3B** top). PfMaf1-FKBP transfected parasite clonal populations were validated for proper integration and confirmation that the system was working, shown by western blot for addition and removal of the ligand, Shield-1, over the course of 3 cycles

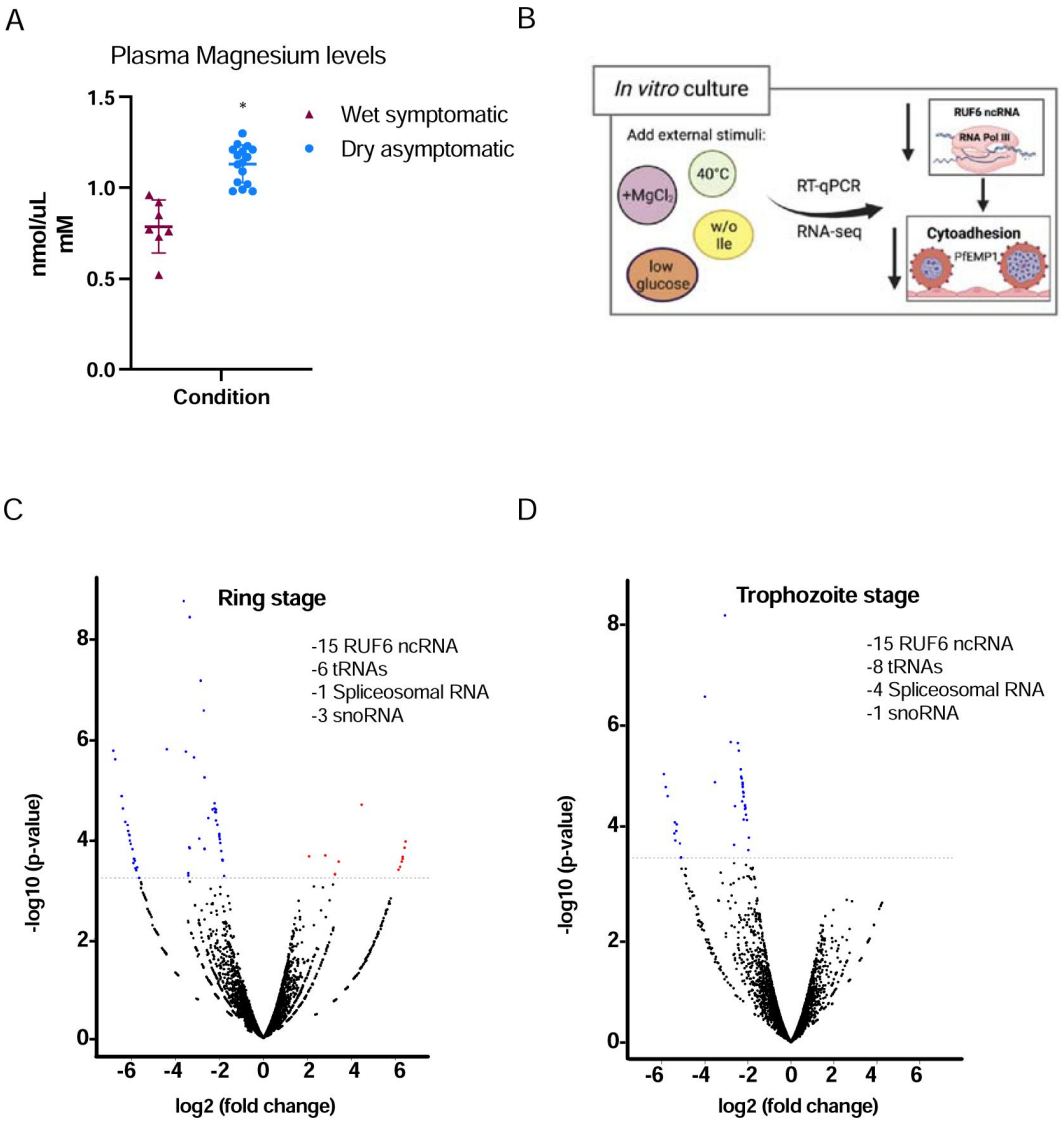

Figure 2.

External factors modulate RNA Pol III-transcribed genes.

(A) Plasma magnesium levels are significantly increased in asymptomatic individuals during the dry season compared to symptomatic individuals during the wet season. Concentration is shown in nmol/μL (mM) (B) Schematic showing underlying molecular mechanism summary using *in vitro* cultured *P. falciparum.* (C, D) Volcano plot showing log2 (fold change, FC) against −log10 (p-value) of transcripts identified by RNA-seq analysis of 3D7 control and addition of $MgCl_2$ harvested during ring (C) and trophozoite stages (D). Expressed transcripts from three replicates between control and addition of $MgCl_2$ that are significantly up-regulated are highlighted in red while significantly down- regulated RNA Pol III genes are highlighted in blue (FDR corrected p-value of <0.05) and a FCL≥±L1.95) with examples listed as text. Black dots indicate non-significant transcripts with a FCL≤L2.0.

(**Figure 3B** bottom). We observed that upon removal of Shield-1, PfMaf1 levels were shown to decrease by approximately 57% in total extracts after one cycle and almost complete degradation was achieved after 2 cycles.

Maf1 in Plasmodium species seemingly affects asexual blood stage proliferation making classical gene KO experiments unattainable (McLean & Jacobs-Lorena, 2017; Zhang *et al*, 2018), pointing to a regulatory role of the putative RNA Pol III inhibitor under normal *in vitro* culture growth conditions. Once PfMaf1 is depleted (**Figure 3B** bottom, 3 cycles - Shield), transcription of tRNA Valine and RUF6 ncRNA increased dramatically by 3-fold (**Figure 3C**), possibly perturbing cellular homeostasis. RNA Pol II-transcribed genes were unaffected. Parasite growth was assessed over the course of 5 days for two PfMaf1-FKBP clones cultured in the presence or absence of PfMaf1 (+/- Shield-1, removed one cycle before day 0, **Figure 3D**). A significant difference in growth was achieved, most evidently in parasites cultured without Shield for 3 cycles, consistent with transposon mutagenesis scoring PfMaf1 essential (Zhang *et al*, 2018). Dead parasites were not detected by Giemsa staining even up to 8 cycles without Shield-1. We confirmed that differences in merozoite numbers per schizont contributed to the change in growth rate between the control and KD PfMaf1 parasites after the 3rd cycle KD (**Figure 3E**).

Additionally, we demonstrated that nuclear PfMaf1 interacts with the RNA Pol III protein complex by performing co-immunoprecipitation followed by quantitative mass spectrometry (Co-IP MS) of cytoplasmic and nuclear fractions of PfMaf1-HA-ddFKBP. Each fraction was split to include a control with no antibody added. Analysis of the quantitative mass spectrometry data revealed unique interactome of cytoplasmic PfMaf1 and nuclear PfMaf1 in their respective samples compared to their controls (**Figure S3A**, B). Gene Ontology (GO) analysis showed that PfMaf1-associated proteins uniquely found in the nuclear fraction, and neither of the two controls nor cytoplasmic fraction, are significantly represented by the biological function category of “RNA Polymerase III transcription” (p = 0.00175) with two subunits of RNA Pol III (Pf3D7_1206600 and Pf3D7_1329000). (GO) analysis of significant and unique proteins found only in the cytoplasmic fractions, and not nuclear, are significantly represented by the molecular function category of “protein kinase activator” (p = 0.0143, Pf3D7_1103100). Additionally, two protein phosphatases (Pf3D7_1127000 and Pf3D7_1464600) were significantly enriched in the cytoplasmic fraction (**Figure S4C**). **Figure 3F** illustrates the cytoplasmic and nuclear enzymes associated with PfMaf1, which could play a role in sensing environmental shifts that lead to the inhibition of Pol III.

Magnesium modulates cytoadhesion through PfMaf1-regulated RNA Pol III transcription

We further investigated if nuclear PfMaf1 activity could be regulated, in response to external factors, to lead to changes in RNA Pol III activity using *P. falciparum* wildtype parasites cultured *in vitro*. The *P. falciparum* cellular localization of PfMaf1 was investigated in response to external stimuli (+$MgCl_2$). Parasites were tightly synchronized, split into control, addition of $MgCl_2$ and harvested during late ring stage. In contrast to several eukaryotic model systems, under normal culture conditions we observed PfMaf1 in cytoplasmic and nuclear fractions using immunoprecipitation followed by western blot analysis (**Figure 4A**, S4A). Nuclear PfMaf1 levels increased upon addition of $MgCl_2$ compared to control nuclear PfMaf1 (**Figure 4A**). Immunofluorescence (IF) assays showed that PfMaf1 forms foci-like aggregates in the cytoplasm and near the nuclear periphery in both culture conditions (**Figure S4B**).

Next, we used the PfMaf1-FKBP transfected parasite lines, to show that the downregulation of RNA Pol III-transcribed genes, triggered by external stimuli, is dependent on PfMaf1. We used the PfMaf1 KD parasites (2nd cycle, see **Figure 3B**) in control conditions and $MgCl_2$ supplementation to the growth medium in ring stage parasites for RT-qPCR (**Figure 4B**). We confirmed the previously observed down-regulation of RNA Pol III-transcribed tRNA Valine and RUF6 upon

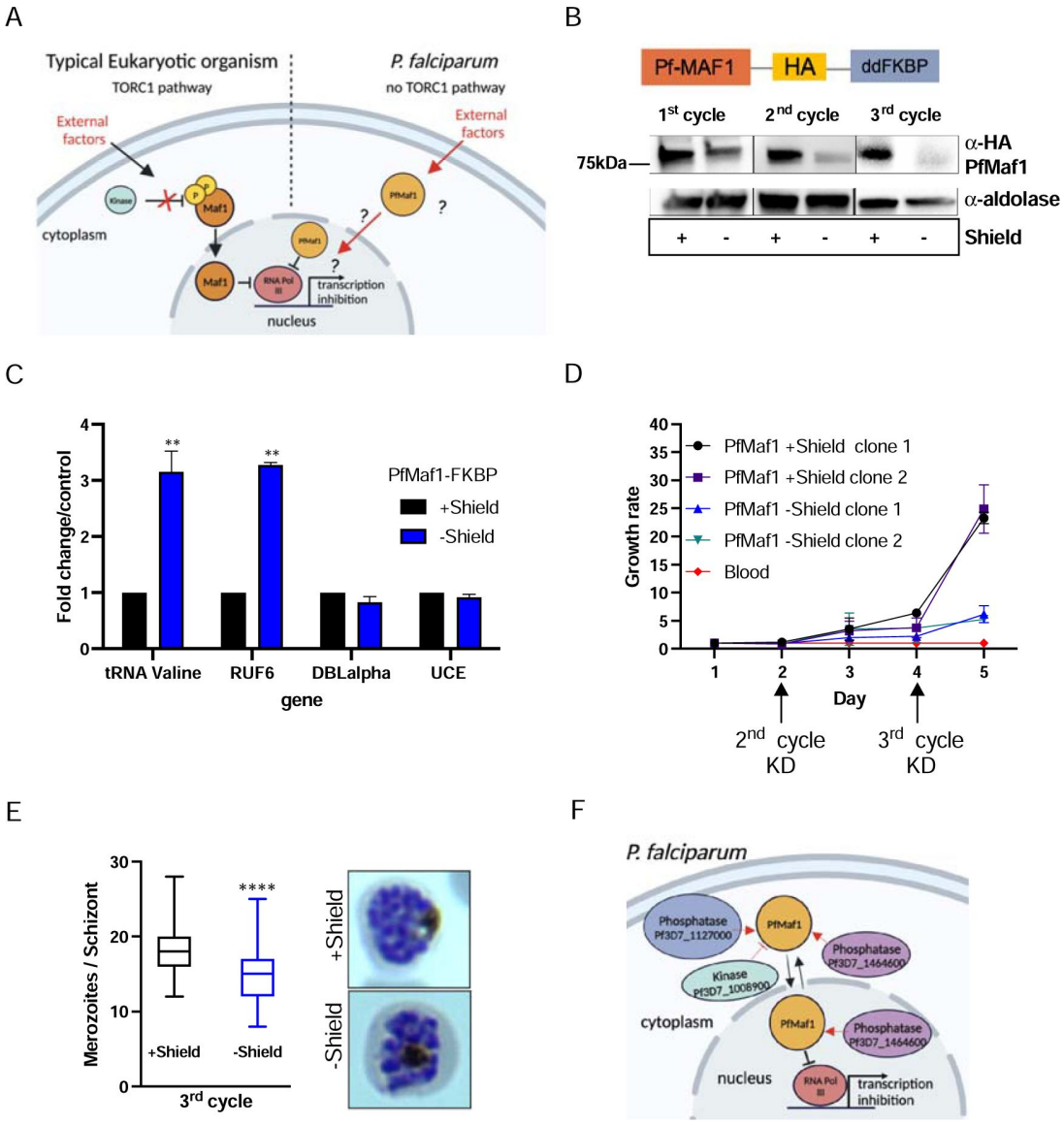

Figure 3.

Nuclear PfMaf1 is essential to regulate RNA Pol III.

(A) Illustration of the TORC1-dependent cellular localization of Maf1 protein in unfavorable conditions in typical eukaryotic organisms compared *P. falciparum* that has no TORC1 pathway. (B, top) Illustration of recombinant PfMaf1 with a 3HA tag followed by a ddFKBP domain to allow for knockdown studies. (B, bottom) Western blot analysis for PfMaf1 in total extracts in pSLI-Maf1-FKBP transfected parasites at 24hpi after 1, 2, and 3 cycles without addition of Shield-1 (-) and control, with addition of Shield-1 (+). Aldolase levels are also shown. Representative of 3 replicates. (C) Transcript levels as quantified by RT-qPCR using the same primers in (**Figure 2B**) in parasites harvested at 18hpi in control group and without Shield for 2 cycles. Error bars are displayed from 3 biological replicates. Statistical significance was determined by two-tailed Student's t-test (** p<0.005). (D) Growth curve over 5 days of clonal pSLI-Maf1-FKBP parasites for 2 conditions: in the presence or absence of Shield-1. Uninfected red blood cells ("blood" in red) serve as reference of background. Error bars indicate standard deviation of three technical replicates in different blood from two different clones (n = 6). (E) Data is represented as box-whisker plot of mean merozoite number per schizont ±SD (Mann-Whitney), with the with the median represented at the center line. Boxplots show the data of 100 segmented schizonts counted per condition (n = 100). Statistical significance was determined by two-tailed Student's t-test (*** p<0.001). Representative giemsa images are shown to the right for + and – Shield. (F) Visual representation of Co-IP MS analysis of cytoplasmic and nuclear PfMaf1. Labeled proteins represent important significant and unique proteins in cytoplasmic and nuclear fractions not found in either of the controls.

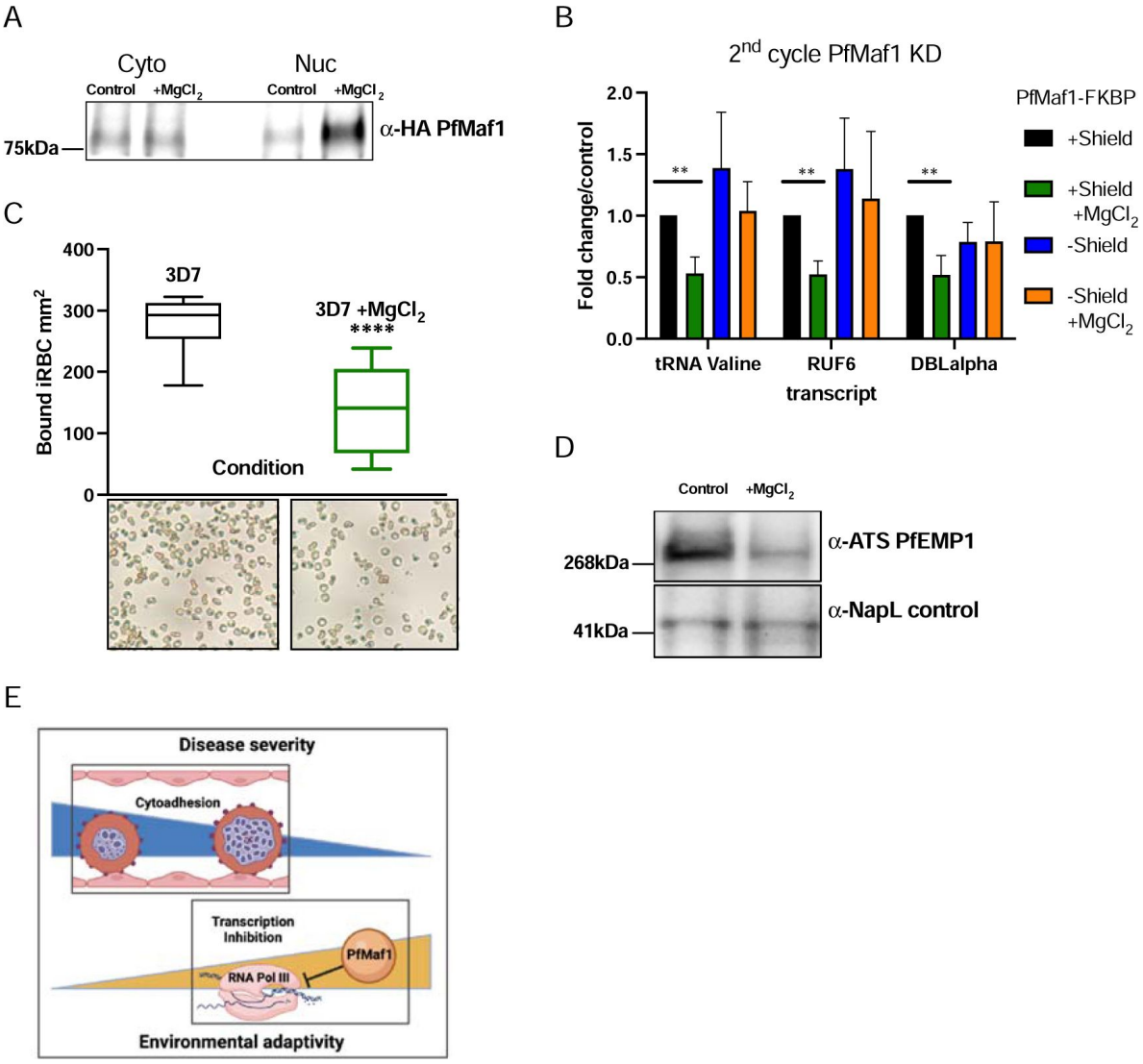

Figure 4.

External factors modulate virulence through PfMaf1-regulated RNA Pol III inhibition

(A) Immunoprecipitation western blot analysis for cytoplasmic and nuclear extracts for PfMaf1 expression in PfMaf1-FKBP transfected parasites with addition of $MgCl_2$ ([3mM] total) and control parasites harvested at 18hpi. Controls are shown in **Figure S4B**. (B) Transcript levels as quantified by RT-qPCR using primers to tRNA Valine (Pf3D7_0312600), RUF6 ncRNA, *var* DBLalpha, and normalized to FBA (Pf3D7_1444800) for 4 conditions: control (black), addition of $MgCl_2$ (green), KD of PfMaf1 (blue), and KD of PfMaf1 and addition of $MgCl_2$ (orange). Error bars are displayed from 3 biological replicates. Statistical significance was determined by two-tailed Student's t-test (** $p<0.005$). (C) Cytoadhesion binding assay data is represented as box-whisker plot of mean number of bound iRBC ±SD (Mann-Whitney) mm^2, with the median represented at the center line. Boxplots show the data of 3 biological replicates (n = 3). Statistical significance was determined by two-tailed Student's t-test (**** $p<0.001$). Representative images are shown below for 3D7 and 3D7 +$MgCl_2$. (D) Western blot analysis for extracts for ATS-PfEMP1 expression in 3D7 control parasites and with addition of $MgCl_2$ ([3mM] total) harvested after plasmion. NapL control levels are also shown. Representative of 3 replicates. (E) Schematic showing summary of study linking decreased cytoadherence, associated with disease severity, with increased RNA Pol III-inhibition, triggered in response to external factors.

$MgCl_2$ supplementation in two independent PfMaf1-FKBP parasite clones. Notably, when PfMaf1 degradation was induced, the addition of $MgCl_2$ did not affect Pol III transcription. These results demonstrate that PfMaf1 mediates the observed decrease in RNA Pol III-transcribed genes with $MgCl_2$ supplementation.

Previous attempts to develop a knockout (KO) line did not yield success, as highlighted by McLean & Jacobs-Lorena in 2017. However, our strain with an inducible system for degrading PfMaf1 protein has unveiled a twofold function of PfMaf1: i) to help maintain Pol III transcription at levels essential for optimal parasite proliferation, and ii) to serve as a key element in an environmental sensing pathway that directly controls Pol III activity.

Finally, we set out to link *P. falciparum* virulence gene expression with decreased RUF6 transcription, by investigating the effect of $MgCl_2$ supplementation on cytoadherence of 3D7 iRBCs. We found that in static binding assays to the endothelial receptor CD36, bound to plastic dishes, adhesion of iRBCs was reduced by 50% with $MgCl_2$ supplementation (**Figure 4C**). This was also confirmed at the protein level using antibodies directed against the conserved intracellular ATS domain of PfEMP1 (**Figure 4D**). Our findings, which demonstrate the inducible inhibition of cytoadhesive capacity, are particularly significant for asymptomatic *P. falciparum* infections, as illustrated in **Figure 4E**.

Discussion

Our study reveals a regulatory mechanism in *P. falciparum* involving RNA Polymerase III, which plays a pivotal role in the parasite's virulence. This discovery illuminates a previously unidentified adaptive molecular process in the parasite's cytoadhesion and proliferation. We propose a connection with asymptomatic infections prevalent during the dry season in African regions, a period characterized by reduced mosquito transmission. In our analysis, we compared RNA from parasites in symptomatic individuals during the wet season to those in asymptomatic individuals in the dry season. In this comparison, we noted a reduction in the levels of tRNAs and RUF6 ncRNA, with the latter being recognized for its involvement in regulating *var* gene expression, as illustrated in **Figures 1A-C**. To date, RNA Polymerase III (Pol III) has not been acknowledged as a factor influencing the virulence of *P. falciparum* in mild or asymptomatic malaria infections. Additionally, our research revealed a link between elevated serum $MgCl_2$ levels and asymptomatic malaria infections, as shown in **Figure 2A**. The normal concentration range for $MgCl_2$ in human serum is between [0.7–1.0mM], while mild hypermagnesemia is characterized by levels ranging from [2.2-3.5mM]. In our pilot study, the average concentration was observed to be around [0.7mM] during the wet season and increased to [1.1mM] in the dry season.

To investigate the potential mechanistic link between the changes in $MgCl_2$ levels and Pol III activity, we established an in vitro culture assay for *P. falciparum* that enabled us to delve into the molecular mechanism underpinning the environment-dependent inhibition of Pol III. We experimented with various concentrations of $MgCl_2$ to assess its effect on Pol III activity. The standard culture medium we used contains [0.5mM] of $MgCl_2$. Our observations indicated a progressive inhibition of Pol III activity in the range of [1-3mM]. To further explore the molecular mechanisms involved, we opted to use a concentration of 3 mmol/L in our continued studies. Quantitative RT-PCR analysis showed inhibition of Pol III transcription of tRNA and the RUF6 ncRNA gene family. Subsequent RNA seq data validated that transcriptional inhibition, induced by $MgCl_2$ supplementation, is primarily limited to canonical RNA Pol III-transcribed genes, which include A and B box containing sequences, and notably the RUF6 gene, crucial for the activation of *var* genes. Our findings established that the inhibition of *var* gene expression, mediated by Pol III, led to a decrease in the cytoadherence of infected red blood cells (iRBCs) when supplemented with $MgCl_2$, as shown in **Figure 4C**. We noted a reduction of over 50% in binding to the endothelial

receptor CD36 in a static binding assay. It is expected that the inhibition of iRBC cytoadherence would be even more pronounced under the physiological shear stress typically found in human capillaries (Crabb *et al*, 1997).

Having established the role of Pol III in the expression of virulence genes, we subsequently showed a link between environmental factors and Maf1, which is the only known eukaryotic repressor of Pol III. We created an inducible system designed to specifically reduce PfMaf1 protein levels, enabling us to explore its influence on Pol III activity. Proteomic analysis through mass spectrometry of PfMaf1's interactome showed its association with various nuclear RNA Pol III subunits, reinforcing its function as a repressor of Pol III in *P. falciparum.* PfMaf1 showed nuclear presence under standard growth conditions. Nuclear shuttling usually increases under specific conditions (stress, nutrient starvation) by changing the phosphorylation state of the Maf1 protein in eukaryotic organisms (Michels *et al*, 2010). Our study supports a model in which a critical baseline amount of PfMaf1 in the nucleus is essential to modulate the expression of tRNAs by RNA Pol III during the multinucleated blood stage of the parasite. This regulation is essential for the parasite to balance its energy resources efficiently while producing large numbers of new infective forms, known as merozoites. Under optimal growth conditions, a single parasite undergoes several rounds of genome replication, forming approximately 30 nuclei within a shared cytoplasm. When PfMaf1 is completely removed, the transcription levels of tRNA Valine and RUF6 ncRNA increase more than threefold, while the transcription level of a Pol II-mediated housekeeping gene UCE remains unchanged. This significant elevation of tRNA transcription beyond physiological levels could potentially lead to an energy deficit within the cell, resulting in the observed reduction in the parasite's multiplication rate, as demonstrated in **Figure 3C and E**. In clinical isolates, parasite densities have been associated with malaria pathogenesis (Nyarko & Claessens, 2021; Thomson-Luque *et al*, 2021) and low parasite densities are also a feature of asymptomatic malaria (Murray *et al*, 2017).

Nutrient availability in the host has been demonstrated to have a profound effect on the replication of parasites using *P. berghei* as a rodent malaria model (Mancio-Silva *et al*, 2017a). Reports from cultured blood stage *P. falciparum* parasites showed that amino acid deficiency can alter parasite growth and survival to stress (McLean & Jacobs-Lorena, 2017; Marreiros *et al*, 2023). Furthermore, a recent report suggested that nutrients involved in S- adenosylmethionine (SAM) metabolism can also affect *var* gene switching in cultured parasites (Schneider *et al*, 2023). Individuals infected with malaria, compared to healthy individuals, were found to have decreased levels (up to 54%) of plasma free amino acids, which could be the result of a nutrient-reduced diet (Leopold *et al*, 2019). In fact, dietary intake, including energy, protein, iron, zinc, calcium and folate, was found to decrease significantly in individuals during the dry season in areas of Africa (M'Kaibi *et al*, 2015). Blood serum magnesium levels can fluctuate in humans and were found to decrease with increasing disease severity (Innocent *et al*, 2013). In our study, plasma magnesium levels were significantly increased in asymptomatic individuals during the dry season compared to symptomatic individuals during the wet season (**Figure 2A**). Wet season samples were within the range of normal serum magnesium levels, whereas dry season samples were higher. It is noteworthy that intracellular magnesium was found to increase in yeast as a result of calorie restriction, defined as a decrease in dietary glucose intake (Abraham *et al*, 2016), indicating that our $MgCl_2$ supplementation could be mimicking low glucose conditions and thus, low nutrient availability. Although interactions between human malaria and malnutrition have been studied for many years, the evidence linking an effect between the two remains inconclusive at the mechanistic level. Our study sets the stage for exploring whether there are additional external stimuli, beyond magnesium chloride, that could activate the regulatory pathway of RNA Polymerase III. Given the lack of a conventional TOR pathway in malaria parasites (Serfontein *et al*, 2010; van Dam *et al*, 2011), the exact signaling pathway that activates PfMaf1 remains unknown. Our mass spectrometry analysis of PfMaf1's cytoplasmic

binding partners has identified interactions with enzymes, such as phosphatases and kinases, which could potentially influence Maf1 activity. This discovery opens up new avenues for future research into the environmental sensing mechanisms that function upstream of PfMaf1.

A traditional view posits that the decreased cytoadherence seen in dry-season parasites may be affected by host immunity, which impairs the parasites' adhesion capabilities. Although experimental evidence supporting this theory is missing, our research introduces a novel perspective to this critical topic by highlighting the role of metabolic changes in modulating virulence gene expression.

In summary, our research demonstrates that RNA Polymerase III activity, regulated by environmental factors, plays a crucial role in the proliferation of parasites and in reducing the cytoadhesive capacity of *P. falciparum.* This discovery unveils a previously unknown molecular process, significantly enhancing our understanding of subclinical parasite persistence. The insights gained from this study could pave the way for novel strategies aimed at preventing severe malaria by promoting reduced pathogen virulence.

Materials and Methods

Parasite and serum samples from malaria infected patients

Venous blood draw of different infected individuals in The Gambia during the dry and wet seasons was collected as previously described in (Collins *et al*, 2022; Fogang *et al*, 2023). The study protocol was reviewed and approved by the Gambia Government/MRC Joint Ethics Committee (SCC 1476, SCC 1318, L2015.50) and by the London School of Hygiene & Tropical Medicine ethics committee (Ref 10982). The field studies were also approved by local administrative representatives, the village chiefs. Written informed consent was obtained from participants over 18 years old and from parents/guardians for participants under 18 years. Written assent was obtained from all individuals aged 12-17 years. The dry season months include January, February, March, April, and May. The wet season months include November and October. For additional information about each sample, see Supplementary Table 2.

Polymerase III inhibition assay

Parasites were treated with 50 µM of RNA Pol III inhibitor CAS 577784-91-9 (Calbiochem, Merck) after sorbitol treatment at 3 ±3hpi and RNA was harvested at 24hpi in parallel with untreated and control samples. The control was treated with the same volume of DMSO added to the inhibitor treated flasks of stock solution.

Clinical isolate RT-qPCR

Total RNA was extracted from TRizol using an miRNeasy minikit and performing on-column DNase treatment (Qiagen) and continued as previously described in ((Collins *et al*, 2022)). Transcript levels were shown by using the following primers: RUF6, Valine tRNA, Asparagine tRNA, and *var* DBLalpha were normalized to the reference gene, fructose- bisphosphate aldolase (PF3D7_1444800, **Figure 2A**, **Table S1**). The starting quantity means from three replicates were extrapolated from a standard curve of serial dilutions of 3D7 genomic DNA.

Plasma magnesium concentration assay

Plasma magnesium levels were determined using a commercial magnesium assay kit (Sigma-Aldrich MAK026) from individuals from the same study as in (Collins *et al*, 2022; Fogang *et al*, 2023). Complete information on tested individual samples can be found in Supplementary Table

2. The protocol was followed as described in the kit and read on a Synergy 2 microplate reader for spectrophotometric reading.

Parasite culture and synchronization

Asexual blood stage 3D7 *P. falciparum* parasites were cultured as previously described in (Lopez-Rubio *et al*, 2009). Parasites were cultured in human RBCs (obtained from the Etablissement Français du Sang with approval number HS 2019-24803) in RPMI-1640 culture medium (Thermo Fisher 11875) supplemented with 10% v/v Albumax I (Thermo Fisher 11020), hypoxanthine (0.1 mM final concentration, C.C.Pro Z-41-M) and 10 mg gentamicin (Sigma G1397) at 4% hematocrit and under 5% O2, 3% CO2 at 37L°C. Static parasite development was monitored by Giemsa staining. Parasites were synchronized by sorbitol (5%, Sigma S6021) lysis at ring stage, plasmagel (Plasmion, Fresenius Kabi) enrichment of late stages 24 h later, and an additional sorbitol lysis 3 h after plasmagel enrichment. The 0 h time point was considered to be 1.5 h after plasmagel enrichment. Parasites were harvested at 1–5% parasitemia.

External stimuli induction

Synchronized parasites were divided into control, addition of magnesium chloride ($MgCl_2$), isoleucine-deficient, low glucose, and 40 degree Celsius and harvested at 18hpi. Parasites exposed to an addition of $MgCl_2$ were supplemented with 0.5mM, 1.5mM, and 2.5 mM $MgCl_2$, for a final concentration of [1mM], [1.5mM], [2mM], and [3mM] including [0.5mM] found in RPMI. Isoleucine-deficient medium consisted of 10.3 g/liter RPMI 1640 isoleucine (Ile) Drop-out medium (United States BioLogicals; catalog no. R9014), supplemented with 2.0 g/liter $NaHCO_3$, 6.0 g/liter HEPES, 10% v/v Albumax I (Thermo Fisher 11020), hypoxanthine (0.1 mM final concentration, C.C.Pro Z-41-M) and 10 mg gentamicin (Sigma G1397). Low glucose (0.25mg/mL) RPMI was made by adding glucose (Dextrose) to glucose-free media: 2.979 g HEPES + 50 mL albumax + 10 mL hypoxanthine + 200 µL gentamycin to final volume of 500 mL with glucose free RPMI (11879). The pH was adjusted to 7.3 with NaOH and filter sterilized. 40-degree Celsius samples were incubated in an adjacent incubator set to 40 degrees Celsius under 5% O2, 3% CO2. Parasites were then harvested with 0.075% Saponin lysis at ~2-5% parasitemia for RNA, genomic DNA, and protein extraction at 18hpi.

RNA isolation and reverse transcription-quantitative PCR (RT-qPCR)

RNA was isolated from synchronized parasite cultures harvested at 18hpi after saponin lysis in 0.075% saponin in PBS, followed by one wash in Dulbecco's phosphate-buffered saline (DPBS, Thermo Fisher 14190) and resuspension in the QIAzol reagent. Total RNA was extracted using an miRNeasy minikit and performing on-column DNase treatment (Qiagen). Reverse transcription from total RNA was achieved using SuperScript VILO (Thermo Fisher Scientific) and random hexamer primers. cDNA levels were quantified by quantitative PCR in the CFX384 real time PCR detection system (BioRad) using Power SYBR Green PCR Master Mix (Applied Biosystems) and primers from a previous study (Guizetti *et al*, 2016). Starting quantity means of three replicates were extrapolated from a standard curve of serial dilutions of genomic DNA. Transcript levels were shown by using the following primers: RUF6, Valine tRNA, Alanine tRNA, Asparagine tRNA, *var* 58 (PF3D7_1240900), and *var* DBLalpha were normalized to the reference gene, fructose-bisphosphate aldolase (PF3D7_1444800).

Stranded RNA sequencing and analysis

Infected RBCs containing synchronized (12 and 24hpi) parasites were lysed in 0.075% saponin (Sigma S7900) in DPBS at 37°C. The parasite cell pellet was washed once with DPBS and then resuspended in 700 µL QIAzol reagent (Qiagen 79306). Total RNA was subjected to rRNA depletion to ensure ncRNA and mRNA capture using the RiboCop rRNA Depletion Kit (Lexogen) prior to

strand-specific RNA-seq library preparation using the TruSeq Stranded RNA LT Kit (Illumina) with the KAPA HiFi polymerase (Kapa Biosystems) for the PCR amplification. Multiplexed libraries were subjected to 150 bp paired-end sequencing on a NextSeq 500 platform (Illumina). Sequenced reads (150 bp paired end) were mapped to the *P. falciparum* genome (Gardner *et al*, 2002) (*plasmoDB.org*, version 3, release 57) using "bwa mem" (Li & Durbin, 2009) allowing a read to align only once to the reference genome (option "–c 1"). Alignments were subsequently filtered for duplicates and a mapping quality ≥ 20 using samtools (Li & Durbin, 2009). Three biological replicates for -$MgCl_2$ and +$MgCl_2$ samples were analyzed for both timepoints.

Generation of PfMaf1 strains

All cloning was performed using KAPA HiFi DNA Polymerase (Roche 07958846001), In- Fusion HD Cloning Kit (Clontech 639649), and XL10-Gold Ultracompetent *E. coli* (Agilent Technologies 200315). Transgenic pSLI parasites were generated as previously described in (Birnbaum *et al*, 2017) with the following modifications: GFP was replaced with a 3HA tag and a ddFKBP domain was added after the protein of interest, PfMaf1. For localization and knock down studies, the last 500-1000 bp of target gene, PfMaf1 Pf3D7_0416500, was cloned into pSLI-3HA-ddFKBP. Each sequence started with an in-frame stop codon but the stop codon at the end of the gene was removed. 50 µg of plasmid DNA was transfected into ring stage 3D7 *P. falciparum* parasites using the protocol described elsewhere (Hasenkamp *et al*, 2013). Transfected parasites were selected with constant drug selection pressure of 2.56 nM WR99210 (Jacobus Pharmaceuticals) to obtain a cell line containing the episomal plasmid. A second drug selection using 400 µg/ml of G418 was done to select for integrants. Once parasites emerged, gDNA of each integration cell line was collected using a commercial kit (DNeasy Blood & Tissue Kit) and checked by PCR to show that integration occurred at the correct locus. Both genome and vector specific primers for the 5' and 3' region were used so that the PCR product would cover the plasmid/genome junction. Vector primers used were the same as described (Birnbaum *et al*, 2017). Once proper size gel bands from PCR were seen, parasites were cloned by limiting dilution, and the targeted genomic locus was sequenced to confirm tag and FKBP integration.

Flow cytometry

Two different pSLI-Maf1-FKBP parasite clones were tightly synchronized and diluted to 0.2% parasitemia (5% hematocrit) at ring stage. One cycle before, Shield-1 was removed from half of the culture. The growth curve was performed in a 96-well plate (200 µl culture per well) with three technical replicates of two biological replicates per condition per clone. At 0 h, 24 h, 48 h, 72 h, and 96 h, 5 µl of the culture was stained in 95 µl of DPBS supplemented with 2× Sybr Green I (Ozyme; stockL=L10,000×) for 30 min at room temperature, diluted 20-fold in D-PBS (final volumeL=L200 µl), and the Sybr Green fluorescence measured in a Guava easyCyte Flow Cytometer (EMD Millipore). 30000 events were counted in duplicate to establish an accurate parasitemia value for each culture. Data was analyzed using the InCyte software (EMD Millipore).

Western blot analysis

Shield-1 was removed for 3 consecutive cycles to monitor the degradation of PfMaf1. Total protein extracts were prepared from trophozoite stages for control and -Shield-1 for 3 cycles. Additionally, membrane extracts were prepared for control and $MgCl_2$ supplementation from parasites isolated from plasmion enrichment. iRBCs were washed once with DPBS at 37°C and lysed with 0.075% saponin (Sigma S7900) in DPBS at 37°C. Parasites were washed once with DPBS, resuspended in 1 ml cytoplasmic lysis buffer (25 mM Tris–HCl pH 7.5, 10 mM NaCl, 1.5 mM MgCl2, 1% IGEPAL CA-630, and 1× protease inhibitor cocktail ["PI", Roche 11836170001]) at 4°C, and incubated on ice for 30 min. Cells were further homogenized with a chilled glass douncer, and the cytoplasmic lysate was cleared with centrifugation (13,500 *g*, 10 min, 4°C). The pellet (containing the nuclei) was resuspended in 100 µl nuclear extraction buffer (25 mM Tris–HCl pH 7.5, 600 mM NaCl, 1.5 mM MgCl2, 1% IGEPAL CA-630, PI) at 4°C and sonicated for 10 cycles with 30 s (on/off) intervals (5 min

total sonication time) in a Diagenode Pico Bioruptor at 4°C. The nuclear lysate was cleared with centrifugation (13,500 *g*, 10Lmin, 4°C). Membrane extracts were prepared by resuspending parasite pellets in NETT buffer (50mM Tris pH8, 150mM NaCl, 5mM EDTA, 1% IGEPAL CA-630, PI) and incubated at 4°C for 10 min. Supernatant was removed after centrifugation (13,500 *g*, 10Lmin, 4°C) and the pellet was resuspended in Tris-saline buffer (50mM Tris pH8, 150mM NaCl, 2% SDS, PI) and sonicated for 6 cycles with 30 s (on/off) intervals (3 min total sonication time) in a Diagenode Pico Bioruptor at 4°C. The membrane lysates were cleared with centrifugation (13,500 *g*, 10Lmin, 4°C). All protein samples were supplemented with NuPage Sample Buffer (Thermo Fisher NP0008) and NuPage Reducing Agent (Thermo Fisher NP0004) and denatured for 5 min at 95°C. Proteins were separated on a 4-15% TGX (Tris-Glycine eXtended) (Bio-Rad) and transferred to a PVDF membrane. The membrane was blocked for 1 h with 5% milk in PBST (PBS, 0.1% Tween 20) at 25°C. HA-tagged proteins, and histone H3 were detected with anti-HA (Abcam 9110, 1:1,000 in 5% milk-PBST) and anti-H3 (Abcam ab1791, 1:1,000 in 5% milk-PBST) primary antibodies, respectively, followed by donkey anti-rabbit secondary antibody conjugated to horseradish peroxidase (“HRP”, Sigma GENA934, 1:5,000 in 5% milk-PBST). Anti-ATS and anti-NapL were detected as previously described (Nacer *et al*, 2015; Dawn *et al*, 2014). Aldolase was detected with anti-aldolase-HRP (Abcam ab38905, 1:5,000 in 5% milk-PBST). HRP signal was developed with SuperSignal West Pico chemiluminescent substrate (Thermo Fisher 34080) and imaged with a ChemiDoc XRS+ (Bio-Rad).

Merozoite number per schizont analysis

Mature schizonts were assessed by microscopic analysis of Giemsa-stained smears and manually quantified using ImageJ software, as reported previously (Marreiros *et al*, 2023). 100 segmented schizonts with clearly individualized merozoites containing a single hemozoin crystal were quantified per condition.

Co-Immunoprecipitation followed by Mass spectrometry (Co-IP-MS)

PfMaf1-HA-ddFKBP tagged parasites (n = 5 biological replicates) were synchronized. At 24hpi, each culture (1.5×10^9 parasites) was centrifuged and RBCs were lysed with six volumes of 0.15% saponin in DPBS for 5 min at 4°C. Parasites were centrifuged at 4,000 *g* for 5 min at 4°C, and the pellet was washed twice with DPBS at 4°C. Parasites were then cross-linked with 1% formaldehyde for 15Lmin at room temperature and quenched with 125 mM glycine for 5 min on ice. Cross-linked parasites were washed twice with DPBS and then resuspended in 900uL of cytoplasmic lysis buffer (10 mM Tris–HCl pH 7.5, 1 mM EDTA, 0.65% IGEPAL CA-630, 10mM NaCl) supplemented with protease inhibitors (Thermo Fisher 78440) at 4°C and incubated with rotation for 30 min at 4°C. Extracts were centrifuged for 10 min at 2000g at 4°C and the cleared cytoplasmic supernatant was removed and kept on ice. The nuclear pellet was resuspended in 900 µL nuclear lysis buffer (10 mM Tris–HCl pH 7.5, 500 mM NaCl, 1 mM EDTA, 1% sodium deoxycholate, 0.1% SDS, 1% IGEPAL CA-630, PI) at 4°C and transferred to 1.5 ml sonication tubes (300 µL per tube, DiagenodeC30010016). Samples were sonicated for 5 min (30 s on/off) in a Diagenode Pico Bioruptor at 4°C. Lysates were then centrifuged for 10 min at 13,500g at 4°C and supernatant was transferred to a fresh tube. Cytoplasmic fractions were mixed with 2:3 ratio of cytoplasmic dilution buffer (10 mM Tris-HCl pH 7.5, 150 mM NaCl, 0.5 mmM EDTA) and nuclear supernatants were mixed with 1:3 ratio of nuclear dilution buffer (10 mM Tris-HCl pH 7.5, 0.5 mmM EDTA). Cytoplasmic and nuclear fraction supernatants were incubated with 1ug of α-HA antibody (Abcam 9110) and 25uL Protein G Magnetic Dynabeads (Invitrogen), pre-incubated for a minimum of 2 hours and washed twice with dilution buffer, overnight with rotation at 4°C. The next day, the beads were collected on a magnet and the supernatant was removed. While on the magnetic stand, beads were washed twice with 500 µL wash buffer (10 mM Tris-HCl pH 7.5, 150 mM NaCl, 0.5 mM EDTA, 0.05% NP40), once with 25LmM NH_4HCO_3 (Sigma 09830) buffer, and then transferred to new tube. Finally, the beads were resuspended in 100 µl of 25LmM NH_4HCO_3 (Sigma 09830) and digested by adding 0.2Lµg of trypsin-LysC (Promega) for 1Lh at 37 °C. Samples were

then loaded into custom-made C18 StageTips packed by stacking one AttractSPE® disk (#SPE-Disks-Bio-C18-100.47.20 Affinisep) in a 200 µL micropipette tip for desalting. Peptides were eluted using a ratio of 40:60 CH3CN:H2OL+L0.1% formic acid and vacuum concentrated to dryness with a SpeedVac apparatus. Peptides were reconstituted in 10 of injection buffer in 0.3% trifluoroacetic acid (TFA) before liquid chromatography-tandem mass spectrometry (LC-MS/MS) analysis. Online LC was performed with an RSLCnano system (Ultimate 3000, Thermo Scientific) coupled to an Orbitrap Eclipse mass spectrometer (Thermo Scientific). Peptides were trapped on a 2 cm nanoviper Precolumn (i.d. 75 µm, C18 Acclaim PepMap^{TM} 100, Thermo Scientific) at a flow rate of 3.0 µL/min in buffer A (2/98 MeCN/H2O in 0.1% formic acid) for 4 min to desalt and concentrate the samples. Separation was performed on a 50 cm nanoviper column (i.d. 75 µm, C18, Acclaim PepMap^{TM} RSLC, 2 µm, 100Å, Thermo Scientific) regulated to a temperature of 50°C with a linear gradient from 2% to 25% buffer B (100% MeCN in 0.1% formic acid) at a flow rate of 300 nL/min over 91 min. MS1 data were collected in the Orbitrap (120,000 resolution; maximum injection time 60 ms; AGC 4 x 10^5). Charges states between 2 and 7 were required for MS2 analysis, and a 60 s dynamic exclusion window was used. MS2 scan were performed in the ion trap in rapid mode with HCD fragmentation (isolation window 1.2 Da; NCE 30%; maximum injection time 60 ms; AGC 104) For identification, the data were searched against the *Homo Sapiens* (UP000005640_9606) and the *Plasmodium falciparum 3D7* (UP000001450_36329) UniProt databases using Sequest HT through proteome discoverer (version 2.4). Enzyme specificity was set to trypsin and a maximum of two miss cleavages sites were allowed. Oxidized methionine, Met-loss, Met- loss-Acetyl and N-terminal acetylation were set as variable modifications. Carbamidomethylation of cysteins were set as fixed modification. Maximum allowed mass deviation was set to 10 ppm for monoisotopic precursor ions and 0.6 Da for MS/MS peaks. The resulting files were further processed using myProMS v3.9.3 (*https://github.com/bioinfo-pf-curie/myproms*) (Poullet *et al*, 2007) FDR calculation used Percolator (The *et al*, 2016) and was set to 1% at the peptide level for the whole study. The label free quantification was performed by peptide Extracted Ion Chromatograms (XICs), reextracted across all conditions and computed with MassChroQ version 2.2.21 (Valot *et al*, 2011) For protein quantification, XICs from proteotypic peptides shared between compared conditions (TopN matching) and missed cleavages were allowed. Median and scale normalization was applied on the total signal to correct the XICs for each biological replicate (n = 5 in each condition). To estimate the significance of the change in protein abundance, a linear model (adjusted on peptides and biological replicates) was performed, and p-values were adjusted using the Benjamini– Hochberg FDR procedure. Proteins with at least 2 distinct peptides in 3 replicates of a same state, a 2-fold enrichment and an adjusted p-value ≤ 0.05 were considered significantly enriched in sample comparisons. Proteins unique to a condition were also considered if they matched the peptides criteria.

Immunofluorescence assay

pSLI-Maf1-FKBP control, +$MgCl_2$ parasites were used with rat anti-HA (Roche 3F10) antibodies. 10 µl of iRBCs were washed with PBS and fixed with for 30 min in 0.0075% Glutaraldehyde/4% PFA/DPBS. After DPBS washing, parasites were permeabilized with 0.1% TritonX100/PBS for 10-15 min before quenching free aldehyde groups with NH_4Cl solution for 10 min. Next, parasites were blocked with 3% BSA–DPBS for 30 min. Primary antibody incubation (1:500 dilution) lasted for 1 h before three washes with PBS, and secondary antibody incubation for 30-60 min, Alexa Fluor 488-conjugated anti-mouse IgG (Invitrogen) diluted 1:2,000 in 4% BSA–DPBS. After three final washes in DPBS, cells were mounted in Vectashield containing DAPI for nuclear staining. Images were captured using a Delta Vision Elite microscope (GE Healthcare). Image overlays were generated using Fiji (Schindelin *et al*, 2012).

Co-Immunoprecipitation followed by western blot (Co-IP-WB)

PfMaf1-HA-ddFKBP tagged parasites were synchronized and split into control and $MgCl_2$ supplementation. At 18hpi, each culture (1.5 × 10^9 parasites) was centrifuged and RBCs were lysed with six volumes of 0.15% saponin in DPBS for 5 min at 4°C. Parasites were centrifuged at 4,000 *g*

for 5 min at 4°C, and the pellet was washed twice with DPBS at 4°C. The parasite pellets were then resuspended in 900uL of cytoplasmic lysis buffer (10 mM Tris–HCl pH 7.5, 1 mM EDTA, 0.65% IGEPAL CA-630, 10mM NaCl) supplemented with protease inhibitors (Thermo Fisher 78440) at 4°C and incubated with rotation for 30 min at 4°C. Extracts were centrifuged for 10 min at 2000g at 4°C and the cleared cytoplasmic supernatant was removed and kept on ice. The nuclear pellet was resuspended in 200 µL nuclear lysis buffer (10 mM Tris–HCl pH 7.5, 500 mM NaCl, 1 mM EDTA, 1% sodium deoxycholate, 0.1% SDS, 1% IGEPAL CA-630, PI) at 4°C and transferred to 1.5 ml sonication tubes (300 µL per tube, DiagenodeC30010016). Samples were sonicated for 5 min (30 s on/off) in a Diagenode Pico Bioruptor at 4°C. Lysates were then centrifuged for 10 min at 13,500g at 4°C and supernatant was transferred to a fresh tube. Cytoplasmic fractions were mixed with 2:3 ratio of cytoplasmic dilution buffer (10 mM Tris-HCl pH 7.5, 150 mM NaCl, 0.5 mmM EDTA) and nuclear supernatants were mixed with 1:3 ratio of nuclear dilution buffer (10 mM Tris-HCl pH 7.5, 0.5 mmM EDTA). Cytoplasmic and nuclear fraction supernatants were incubated with 1ug of α-HA antibody (Abcam 9110) and 25uL Protein G Magnetic Dynabeads (Invitrogen), pre-incubated for a minimum of 2 hours and washed twice with dilution buffer, overnight with rotation at 4°C. The next day, the beads were collected on a magnet and the supernatant was removed. While on the magnetic stand, beads were washed twice with 500 µL wash buffer (10 mM Tris-HCl pH 7.5, 150 mM NaCl, 0.5 mM EDTA, 0.05% NP40), once with 25LmM NH_4HCO_3 (Sigma 09830) buffer, and then transferred to new tube. Finally, the beads were resuspended in 20µl 2x SDS sample buffer and reducing agent before 5 min at 95°C. The beads were separated with magnet and the supernatant was transferred to a new tube. Western blot protocol was followed as mentioned earlier.

Static cytoadhesion binding assay

Mature stage iRBCs for 3D7 control and supplementation of $MgCl_2$ ([3mM] total concentration) for 1 cycle were used for cytoadhesion binding assays. Receptors diluted in PBS (10 µg/mL target CD36 or negative control 1% BSA) were incubated overnight at 4°C in labeled petri dishes. After the dishes were blocked for 30 minutes at 37°C with 1% BSA/PBS, parasitemia was measured with a Guava easyCyte Flow Cytometer (EMD Millipore) after trophozoites and schizonts iRBCs were isolated by plasmagel (Plasmion, Fresenius Kabi) enrichment. Adjusted amounts of iRBCs were resuspended in binding medium (RPMI 1640 powder (Gibco 51800: W/L-Glutamine W/O $NaHCO_3$) with HEPES pH 7) for a concentration of 2.2×10^8 iRBCs/mL. iRBCs/binding medium was added to each petri dish and incubated for 2 hours at 37°C. After, unbound cells were removed and the dishes were washed 5 times with binding medium by carefully tilting from side to side. Adherent iRBCs were counted using 40x lens with a Nikon ECLIPSE TE200 in 10 randomly selected fields (each with 0.2 μm^2) before 2 our fixation with 2% glutaraldehyde (G5882; Sigma)/PBS. After fixation, giemsa staining was done to confirm percentage of bound iRBCs. A total of 3 biological replicates were performed and the results were expressed as the number of bound iRBCs per 0.2 mm^2 of target receptor monolayer.

Statistical analysis

All statistical analyses were performed using GraphPad Prism version 9.1.0 (216) for Mac. To test for a normal distribution of the data, the Shapiro-Wilk normality test was used. To test for significance between two groups, a two-sided independent-samples t test was used. Gene ontology enrichments were calculated using the build-in tool at *https://plasmoDB.org*.

Estimation of cell cycle progression

RNA-seq-based cell cycle progression for control and $MgCl_2$ supplementation was estimated in R by comparing the normalized expression values (i.e., RPKM, reads per kilobase per exon per one million mapped reads) of each sample to the microarray data from Bozdech et al (2003) (Data ref: Bozdech et al, 2003) using the statistical model as in Lemieux et al (2009).

Data availability

The data generation in this study is available in the following database:

The mass spectrometry proteomics data have been deposited to the ProteomeXchange Consortium via the PRIDE (Perez-Riverol *et al*, 2022) partner repository with the dataset identifier PXD040576" (Username: reviewer_pxd040576@ebi.ac.uk & Password: wlw5Mlc6).

Acknowledgements

We thank L. Mancio Silva, E. Real and J. Bryant for critical reading this manuscript. This work was supported by the Laboratoire d'Excellence (LabEx) ParaFrap [ANR-11-LABX- 0024], ERC AdG PlasmoSilencing (670301), ANR-JC (18-CE15-0009-01). We thank Camille Cohen and Marta Miera Maluenda for technical assistance with this project. With financial support from "la Région Île-de-France" (N°EX061034) and ITMO Cancer of Aviesan and INCa on funds administered by Inserm (N°21CQ016-00) for MS analysis.

Author contributions

Conceptualization A.S, GD; Methodology: GD, AClaës, AB, PBN; Investigation GD, AClaës, AB; Analysis: GD, AB, FD, DL; Writing: GD and A.S; Funding acquisition: A.S, AC

Conflict of interest

The funders had no role in the study design, data collection, and interpretation or decision to submit the work for publication. The authors declare that they have no conflict of interest.

A

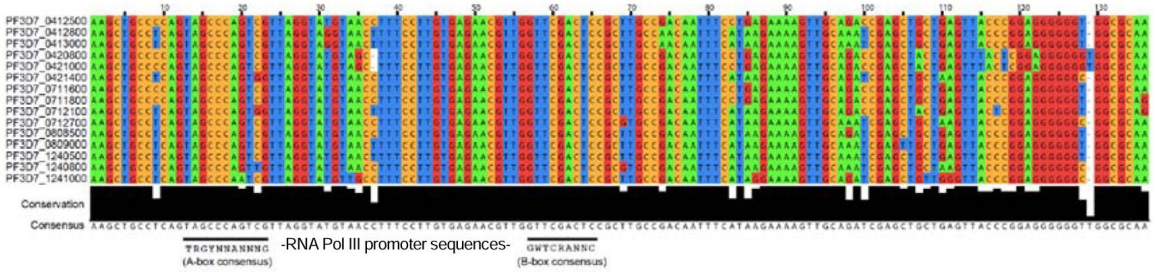

B

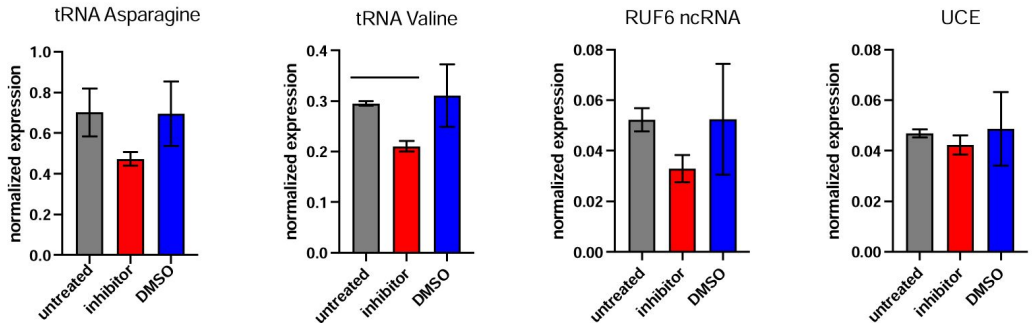

Figure S1.

(A) Multiple sequence alignment of highly conserved genes encoding GC-rich ncRNA elements. 15 members of RUF6 gene family aligned by Clustal Omega (*http://www.ebi.ac.uk*) and presented in Jalview (*http://www.jalview.org*). Degree of conservation per base and consensus sequence are displayed below. Black lines show position of potential A- and B-box consensus motifs (as assessed in (Guizetti *et al*, 2016)). (B) RT- qPCR shows transcript levels for tRNA Asparagine, tRNA Valine, RUF6 ncRNA and a housekeeping gene encoding ubiquitin-conjugating enzyme in synchronized wildtype parasites at 24 hpi that were untreated or treated with RNA Pol III inhibitor or DMSO. Transcript levels are normalized to fructose-bisphosphate aldolase (PF3D7_1444800) transcript levels. MeanLSEM of two independent experiments are shown. Statistical significance was determined by two-tailed Student's t-test (* $p<0.05$).

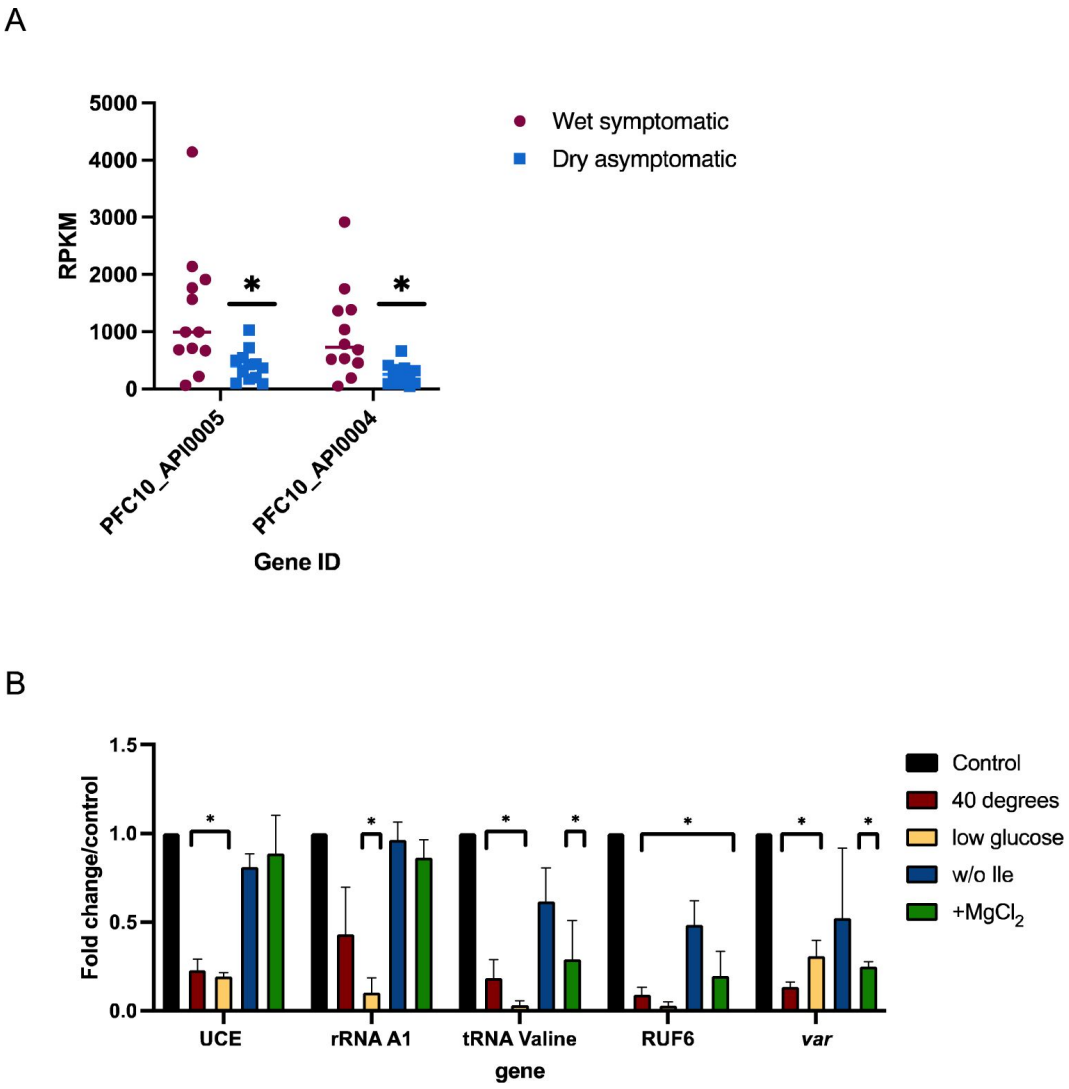

Figure S2.

(A) tRNA Leucine (Pf3D7_API05400) and tRNA Asparagine (Pf3D7_API05500) transcripts identified by RNA-Seq analysis from ((Andrade *et al*, 2020)) for wet symptomatic (n = 12) and dry asymptomatic (n = 12) individuals. Statistical significance was determined by two-tailed Student's t-test (* p<0.05). (B) Transcript levels as quantified by RT-qPCR on 3D7 parasites harvested during late ring stage for control parasites, parasites in the absence of isoleucine (w/o Ile), at 40 degrees Celsius, at low-glucose levels (0.5mg/mL), and presence of additional $MgCl_2$ ([3mM] total). Primers were used for Pol II-transcribed ubiquitin- conjugating enzyme (UCE Pf3D7_0812600), Pol I-transcribed rRNA A1, Pol III-transcribed RUF6 ncRNA, Pol III-transcribed tRNA Valine (Pf3D7_0312600), and Pol II-transcribed active *var* gene (Pf3D7_1240900). Results are normalized to an RNA Pol II-transcribed reference gene FBA (Pf3D7_1444800) and presented as fold change/control. Error bars are displayed from 3 biological replicates. Statistical significance was determined by two-tailed Student's t-test (* p<0.05).

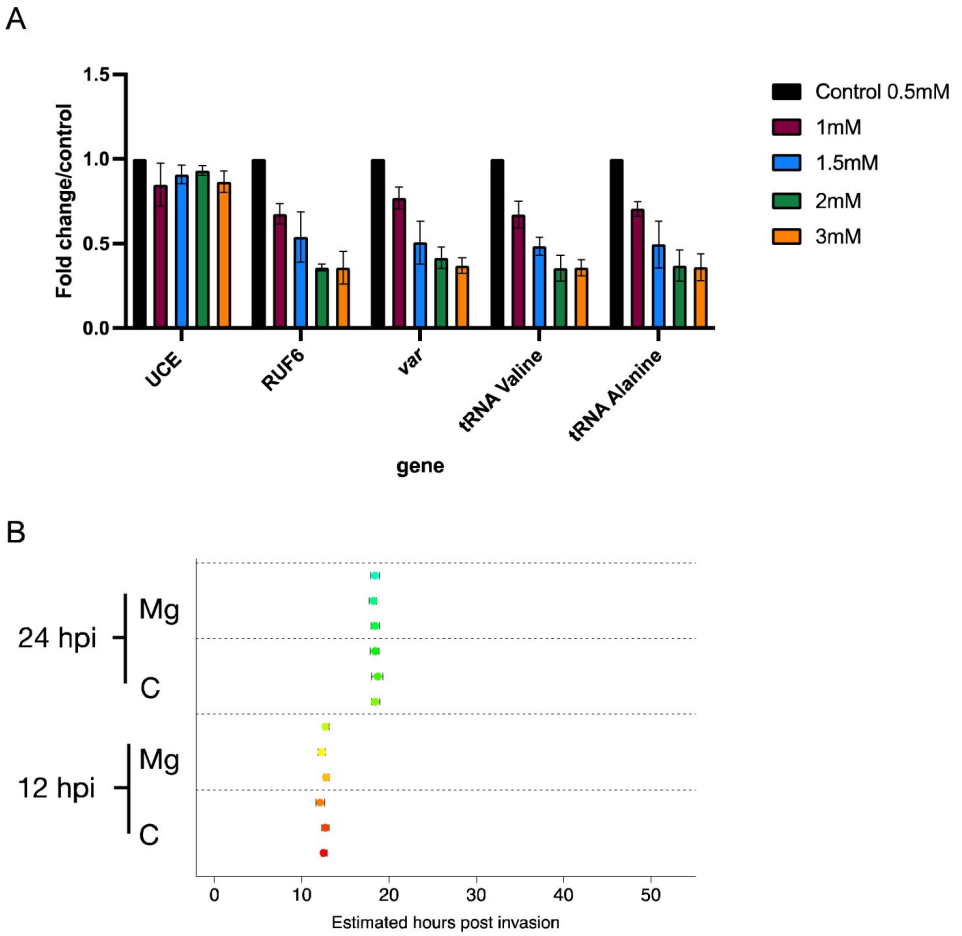

Figure S3.

(A) Transcript levels as quantified by RT-qPCR on 3D7 parasites harvested during late ring stage for control parasites and parasites in the presence of additional $MgCl_2$ levels ([1mM], [1.5mM], [2mM], and [3mM] total). Primers were used for Pol II-transcribed ubiquitin-conjugating enzyme (UCE Pf3D7_0812600), Pol III- transcribed RUF6 ncRNA, Pol III-transcribed tRNA Valine (Pf3D7_0312600) and Alanine (PF3D7_0411500), and Pol II-transcribed *var* DBLalpha. Results are normalized to an RNA Pol II-transcribed reference gene FBA (Pf3D7_1444800) and presented as fold change/control. Error bars are displayed from 3 biological replicates. (B) Cell cycle progression estimation of a wildtype 3D7 clone in the absence ('C') or presence ('Mg') of $MgCl_2$ supplementation. RNA-seq data from synchronized parasites harvested at 12 and 24 hpi were compared to microarray data (from (Bozdech *et al*, 2003) as in (Lemieux *et al*, 2009). Replicates are represented with circles.

A Cytoplasmic PfMaf1 vs Cytoplasmic Control

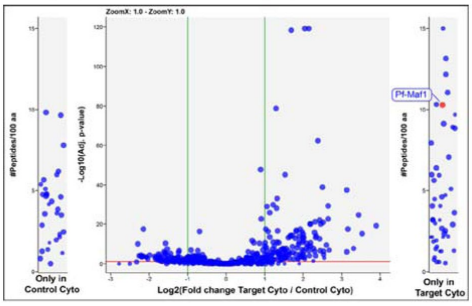

B Nuclear PfMaf1 vs Nuclear Control

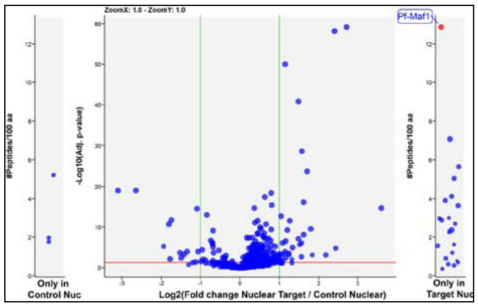

C

Gene ID	Ab Cytoplasm/Control Cytoplasm						Total peptides in set	MW (kDa)	Description
	Ratio	Log2(Ratio)	Adj. p-value	Dist. pept. used	Pept. used	Distrib. dist. pep. in replic.			
PF3D7_1464600	2,263481181	1,178543312	1,577E-06	6	31	4, 5, 5, 4, 3/0, 4, 3, 2, 1	70	170,5	Serine/threonine protein phosphatase UIS2, putative
PF3D7_1127000	2,838513427	1,505135586	0,00160101	2	16	1, 2, 2, 2, 2/1, 0, 2, 2, 2	17	34,5	Protein phosphatase, putative

Gene ID	Ab Nuclear/Control Nuclear						Total peptides in set	MW (kDa)	Description
	Ratio	Log2(Ratio)	Adj. p-value	Dist. pept. used	Pept. used	Distrib. dist. pep. in replic.			
PF3D7_0507700	4,544185096	2,184021601	0,00072787	3	18	3, 2, 3, 2, 2/2, 0, 2, 0, 2	32	62,6	Nuclear protein localization protein 4, putative
PF3D7_1206600	1000	1000		6	13	2, 3, 3, 3, 2/0, 0, 0, 0, 0	13	167,3	DNA-directed RNA polymerase subunit beta
PF3D7_1329000	1000	1000		5	13	2, 3, 1, 3, 2/1, 1, 0, 0, 0	13	274,8	DNA-directed RNA polymerase subunit

D

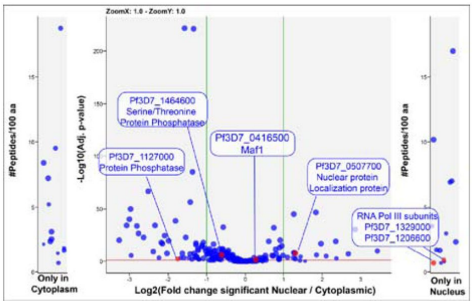

Figure S4.

PfMaf1 cytoplasmic and nuclear interactome.

Co-IP MS volcano plot of enrichment for all 5 replicates for cytoplasmic (A) and nuclear (B) PfMaf1 vs control proteins are indicated and labeled. Each dot represents a protein, and its size corresponds to the sum of peptides from both conditions used to quantify the ratio of enrichment. *x*-axis = $\log_2$(fold-change), *y*-axis = $-\log_{10}$(p-value), horizontal red line indicates adjusted p- value = 0.05, and vertical green lines indicate absolute fold-change = 2.0. Side panels indicate proteins uniquely identified in either sample (*y*-axis = number of peptides per 100 amino acids) with a minimum of 2 distinct peptides in 3 replicates of a same state. (C) Table showing values for significantly and uniquely enriched proteins from both extracts as labeled in (**Figure 3F**). (D) Volcano plot showing the distribution of significant and unique proteins in cytoplasmic and nuclear fractions not found in either of the controls. Each dot represents a protein, and its size corresponds to the sum of peptides from both conditions used to quantify the ratio of enrichment. *x*-axis = $\log_2$(fold-change), *y*-axis = $-\log_{10}$(p-value), horizontal red line indicates adjusted p- value = 0.05, and vertical green lines indicate absolute fold-change = 2.0. Side panels indicate proteins uniquely identified in either sample (*y*-axis = number of peptides per 100 amino acids) with a minimum of 2 distinct peptides in 3 replicates of a same state.

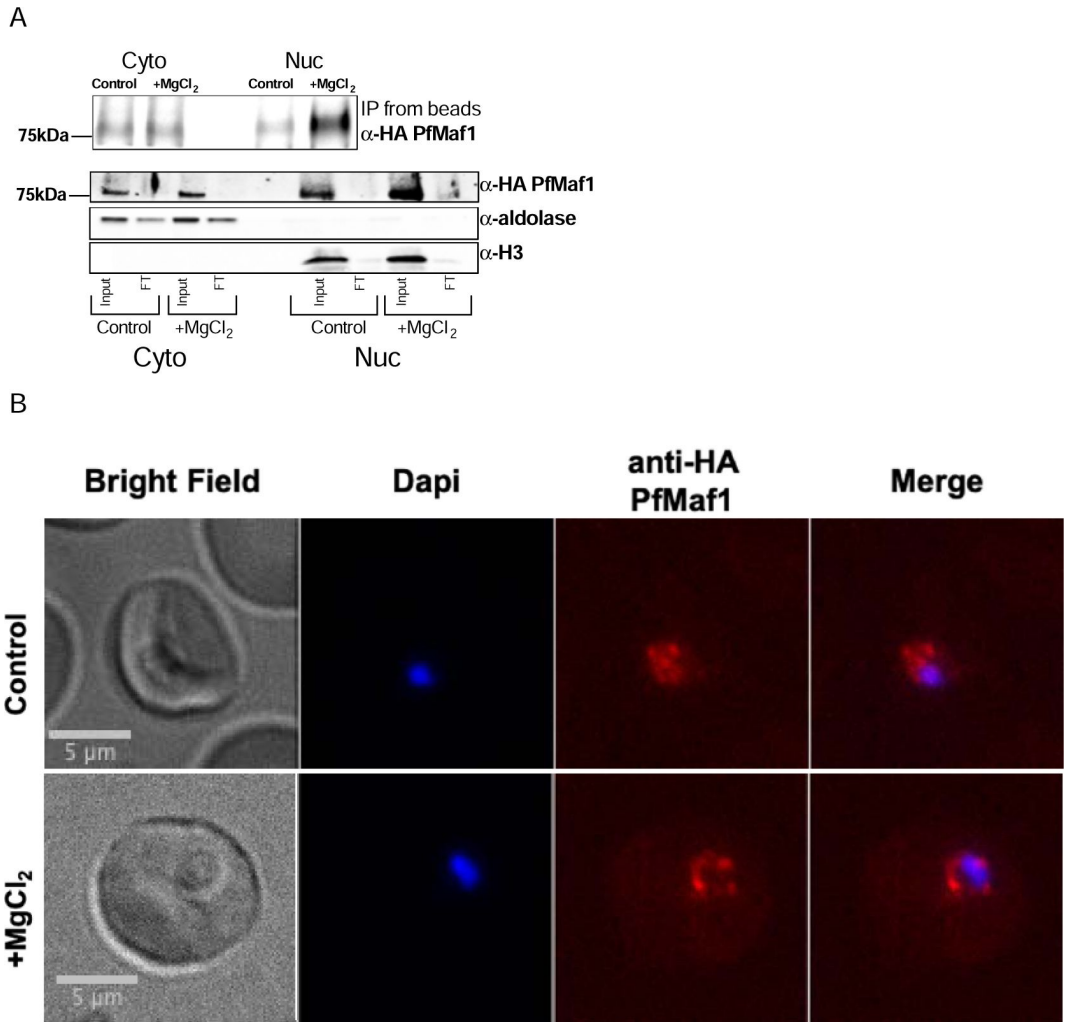

Figure S5.

(A) Immunoprecipitation western blot analysis for cytoplasmic and nuclear extracts for PfMaf1 expression in PfMaf1-FKBP transfected parasites with addition of $MgCl_2$ ([3mM] total) and control parasites harvested at 18hpi from **Figure 4A**. Anti-HA PfMaf1, aldolase and histone H3 are shown from input and flow- through (FT). (B) Representative immunofluorescence images show brightfield, Dapi, anti-HA PfMaf1, and Dapi-HA merge for PfMaf1 in control and addition of $MgCl_2$ ([3mM] total) in parasites harvested and fixed at late ring stage.

Primer pair	Forward	Reverse
Pool RUF6 A RUF6 B	5'-AAGCTGCCTCAGTAGCCCA-3'	5'-AAAAATTGCGCCACCCCC-3'
	5'-AAGCTGCCCCAGTAGCCCA-3'	5'-AAAAATTGCGCCGCCCCC-3'
rRNA A1 (from (Mancio-Silva *et al*, 2010))	5'-TGTTTTCTTTTTTCTAAGTTT-3'	5'-TCACCTCATTTGAAGCAA-3'
tRNA Alanine (PF3D7_0411500)	5'-GGGCAGGTGGTGTAGTGG-3'	5'-TGCTGGACAGACGGGGAATT-3'
tRNA Asparagine (PF3D7_0714700)	5'-GCAAGTATTTCCGCCTGTCA-3'	5'-GAATTGAACCCGGGTCTTCC-3'
tRNA Valine (Pf3D7_0312600)	5'-GCGGGCATGGTCTAGTGG-3'	5'-ACTACGGGCACCGAGGATC-3'
FBA fructose-bisphosphate aldolase (PF3D7_1444800)	5'-TGTACCACCAGCCTTACCAG-3'	5'-TTCCTTGCCATGTGTTCAAT-3'
UCE ubiquitin-conjugating enzyme (Pf3D_70812600)	5'-TAACAGCCCAGCGAATCAAG-3'	5'-CGGCATCTTCTTCAGCTTTCTG-3'
var gene (PF3D7_1240900)	5'-CAAAATGGTAGTGATGGTGGTCG-3'	5'-CCCCCTGCTTTATTATCTTTCGTC-3'
Pool *var* DBLalpha	5'-GCACGAACTTTTGCA-3'	5'-GCCCCATTCGTCGAACC-3'
	5'-GCACGCAGTTTTGCA-3'	5'-GCCCCATTCCTCGAACC-3'

Supplementary Table 1.

qPCR analysis primer pairs

References

1. Abraham KJ *et al.* (2016) **Intersection of calorie restriction and magnesium in the suppression of genome-destabilizing RNA-DNA hybrids** *Nucleic Acids Res Oct* **14**:44–18

2. Andrade CM, Fleckenstein H, Thomson-Luque R (2020) **Increased circulation time of Plasmodium falciparum underlies persistent asymptomatic infection in the dry season** *Nat Med* **26**:1929–1940

3. Babbitt SE, Altenhofen L, Cobbold SA, Istvan ES, Fennell C, Doerig C, Llinás M, Goldberg DE (2012) **Plasmodium falciparum responds to amino acid starvation by entering into a hibernatory state** *Proc Natl Acad Sci USA*

4. Barcons-Simon A, Cordon-Obras C, Guizetti J, Bryant JM, Scherf A (2020) **CRISPR Interference of a Clonally Variant GC-Rich Noncoding RNA Family Leads to General Repression of var Genes in Plasmodium falciparum** *mBio*

5. Birnbaum J, Flemming S, Reichard N (2017) **A genetic system to study Plasmodium falciparum protein function** *Nat Methods* **14**:450–456

6. Bozdech Z, Llinás M, Pulliam BL, Wong ED, Zhu J, DeRisi JL (2003) **The Transcriptome of the Intraerythrocytic Developmental Cycle of Plasmodium falciparum** *PLoS Biol* **1**

7. Collins KA *et al.* (2022) **A Cohort Study on the Duration of Plasmodium falciparum Infections During the Dry Season in The Gambia** *The Journal of Infectious Diseases* **226**:128–137

8. Crabb BS, Cooke BM, Reeder JC, Waller RF, Caruana SR, Davern KM, Wickham ME, Brown GV, Coppel RL, Cowman AF (1997) **Targeted Gene Disruption Shows That Knobs Enable Malaria-Infected Red Cells to Cytoadhere under Physiological Shear Stress** *Cell* **89**:287–296

9. van Dam TJP, Zwartkruis FJT, Bos JL, Snel B (2011) **Evolution of the TOR Pathway** *J Mol Evol* **73**:209–220

10. Dawn A, Singh S, More KR, Siddiqui FA, Pachikara N, Ramdani G, Langsley G, Chitnis CE (2014) **The Central Role of cAMP in Regulating Plasmodium falciparum Merozoite Invasion of Human Erythrocytes** *PLoS Pathog* **10**

11. Diffendall GM, Barcons-Simon A, Baumgarten S, Dingli F, Loew D, Scherf A (2022) **Discovery of RUF6 ncRNA–interacting proteins involved in P. falciparum immune evasion** *Life Sci Alliance* **6**

12. Fan Y *et al.* (2020) **Rrp6 Regulates Heterochromatic Gene Silencing via ncRNA RUF6 Decay in Malaria Parasites** *mBio* **11**:e01110–20

13. Fang J, Sullivan M, McCutchan TF (2004) **The Effects of Glucose Concentration on the Reciprocal Regulation of rRNA Promoters in Plasmodium falciparum** *Journal of Biological Chemistry* **279**:720–725

14. Fogang B *et al.* (2023) **Asymptomatic Plasmodium falciparum Carriage at the End of the Dry Season is Associated with Subsequent Infection and Clinical Malaria in Eastern Gambia Epidemiology**

15. Gardner MJ *et al.* (2002) **Genome sequence of the human malaria parasite Plasmodium falciparum** *Nature* **419**:498–511

16. Guillochon E *et al.* (2022) **Transcriptome Analysis of Plasmodium falciparum Isolates From Benin Reveals Specific Gene Expression Associated With Cerebral Malaria** *The Journal of Infectious Diseases* **225**:2187–2196

17. Guizetti J, Barcons-Simon A, Scherf A (2016) **Trans-acting GC-rich non-coding RNA at var expression site modulates gene counting in malaria parasite** *Nucleic Acids Res* **44**:9710–9718

18. Guizetti J, Scherf A (2013) **Silence, activate, poise and switch! Mechanisms of antigenic variation in Plasmodium falciparum** *Cell Microbiology* **15**:718–726

19. Hasenkamp S, Merrick CJ, Horrocks P (2013) **A quantitative analysis of Plasmodium falciparum transfection using DNA-loaded erythrocytes** *Mol Biochem Parasitol* **187**:117–120

20. Hess FI, Kilian A, Söllner W, Nothdurft HD, Pröll S, Löscher T (1995) **Plasmodium falciparum and Plasmodium berghei: Effect of Magnesium on the Development of Parasitemia** *Experimental Parasitology* **80**:196–193

21. Innocent O, Ejovi O, Charles E (2013) **Levels of iron and magnesium in serum of Plasmodium falciparum malarial infected children in Abraka, Delta State** *Nigeria. J Invest Biochem* **2**

22. Jahnen-Dechent W, Ketteler M (2012) **Magnesium basics** *Clinical Kidney Journal* **5**:i3–i14

23. Jensen MD, Conley M, Helstowski LD (1983) **Culture of Plasmodium falciparum: The Role of pH, Glucose, and Lactate** *The Journal of Parasitology* **69**

24. Kimenyi KM, Wamae K, Ochola-Oyier LI (2019) **Understanding P. falciparum Asymptomatic Infections: A Proposition for a Transcriptomic Approach** *Front Immunol* **10**

25. Kumar M, Skillman K, Duraisingh MT (2021) **Linking nutrient sensing and gene expression in Plasmodium falciparum blood-stage parasites** *Mol Microbiol* **115**:891–900

26. Leech JH, Barnwell JW, Miller LH, Howard RJ (1984) **Identification of a strain-specific malarial antigen exposed on the surface of plasmodium falciparum-infected erythrocytes** *J Exp Med* **159**:1567–1575

27. Lemieux JE *et al.* (2009) **Statistical estimation of cell-cycle progression and lineage commitment in Plasmodium falciparum reveals a homogeneous pattern of transcription in ex vivo culture** *Proc Natl Acad Sci USA* **106**:7559–7564

28. Leopold SJ *et al.* (2019) **Amino acid derangements in adults with severe falciparum malaria** *Sci Rep* **9**

29. Li H, Durbin R (2009) **Fast and accurate short read alignment with BurrowsWheeler transform** *Bioinformatics* **25**:1754–1760

30. Lopez-Rubio JJ, Mancio-Silva L, Scherf A (2009) **Genome-wide analysis of heterochromatin associates clonally variant gene regulation with perinuclear repressive centers in malaria parasites** *Cell Host Microbe* **5**:179–190

31. Mancio-Silva L *et al.* (2017) **Nutrient sensing modulates malaria parasite virulence** *Nature* **547**:213–216

32. Mancio-Silva L *et al.* (2017) **Nutrient sensing modulates malaria parasite virulence** *Nature* **547**:213–216

33. Mancio-Silva L, Zhang Q, Scheidig-Benatar C, Scherf A (2010) **Clustering of dispersed ribosomal DNA and its role in gene regulation and chromosome-end associations in malaria parasites** *Proc Natl Acad Sci USA* **107**:15117–15122

34. Marreiros IM, Marques S, Parreira A, Mastrodomenico V, Mounce BC, Harris CT, Kafsack BF, Billker O, Zuzarte-Luís V, Mota MM (2023) **A non-canonical sensing pathway mediates Plasmodium adaptation to amino acid deficiency** *Commun Biol* **6**

35. McLean KJ, Jacobs-Lorena M (2017) **Plasmodium falciparum Maf1 Confers Survival upon Amino Acid Starvation** *mBio* **8**:2317–16

36. Michels AA, Robitaille AM, Buczynski-Ruchonnet D, Hodroj W, Reina JH, Hall MN, Hernandez N (2010) **mTORC1 Directly Phosphorylates and Regulates Human MAF1** *Mol Cell Biol* **30**:3749–3757

37. Miller LH, Ackerman HC, Su X, Wellems TE (2013) **Malaria biology and disease pathogenesis: insights for new treatments** *Nat Med* **19**:156–167

38. Miller LH, Baruch DI, Marsh K, Doumbo OK (2002) **The pathogenic basis of malaria** *Nature* **415**:673–679

39. M'Kaibi FK, Steyn NP, Ochola S & Du Plessis L (2015) **Effects of agricultural biodiversity and seasonal rain on dietary adequacy and household food security in rural areas of Kenya** *BMC Public Health* **15**

40. Murray L, Stewart LB, Tarr SJ, Ahouidi AD, Diakite M, Amambua-Ngwa A, Conway DJ (2017) **Multiplication rate variation in the human malaria parasite Plasmodium falciparum** *Sci Rep* **7**

41. Nacer A, Claes A, Roberts A, Scheidig-Benatar C, Sakamoto H, Ghorbal M (2015) **Discovery of a novel and conserved Plasmodium falciparum exported protein that is important for adhesion of PfEMP1 at the surface of infected erythrocytes** *Cell Microbiol* **17**:1205–1216

42. Nyarko PB, Claessens A (2021) **Understanding Host–Pathogen–Vector Interactions with Chronic Asymptomatic Malaria Infections** *Trends in Parasitology* **37**:195–204

43. Perez-Riverol Y *et al.* (2022) **The PRIDE database resources in 2022: a hub for mass spectrometry-based proteomics evidences** *Nucleic Acids Research* **50**:D543–D552

44. Pluta K, Lefebvre O, Martin NC, Smagowicz WJ, Stanford DR, Ellis H SR, A B AK S (2001) **Maf1p, a negative effector of RNA polymerase III in Saccharomyces cerevisiae** *Mol Cell Biol* **21**:5031–5040

45. Poullet P, Carpentier S, Barillot E (2007) **myProMS, a web server for management and validation of mass spectrometry-based proteomic data** *Proteomics* **7**:2553–2556

46. Rollins J, Veras I, Cabarcas S, Willis I, Schramm L (2007) **Human Maf1 negatively regulates RNA Polymerase III transcription via the TFIIB family members Brf1 and Brf2** *Int J Biol Sci* :292–302

47. Scherf A, Hernandez-Rivas R, Buffet P, Bottius E, Benatar C, Pouvelle B, Gysin J, Lanzer M (1998) **Antigenic variation in malaria: in situ switching, relaxed and mutually exclusive transcription of var genes during intra-erythrocytic development in Plasmodium falciparum** *EMBO J* **17**:5418–5426

48. Schindelin J *et al.* (2012) **Fiji: an open-source platform for biological-image analysis** *Nat Methods* **9**

49. Schneider VM *et al.* (2023) **The human malaria parasite Plasmodium falciparum can sense environmental changes and respond by antigenic switching** *Proc Natl Acad Sci USA* **120**

50. Serfontein J, Nisbet RER, Howe CJ, de Vries PJ (2010) **Evolution of the TSC1/TSC2-TOR Signaling Pathway** *Sci Signal*

51. Smith JD, Chitnis CE, Craig AG, Roberts DJ, Hudson-Taylor DE, Peterson DSP R. N, Miller LH (1995) **Switches in expression of plasmodium falciparum var genes correlate with changes in antigenic and cytoadherent phenotypes of infected erythrocytes** *Cell* **82**:101–110

52. Smith JD, Rowe JA, Higgins MK, Lavstsen T (2013) **Malaria's deadly grip: cytoadhesion of Plasmodium falciparum-infected erythrocytes: Plasmodium falciparum cytoadhesion and var genes** *Cell Microbiol* **15**:1976–1983

53. The M, MacCoss MJ, Noble WS, Käll L (2016) **Fast and Accurate Protein False Discovery Rates on Large-Scale Proteomics Data Sets with Percolator 3.0** *J Am Soc Mass Spectrom* **27**:1719–1727

54. Thomson-Luque R *et al.* (2021) **Plasmodium falciparum transcription in different clinical presentations of malaria associates with circulation time of infected erythrocytes** *Nat Commun* **12**

55. Valot B, Langella O, Nano E, Zivy M (2011) **MassChroQ: a versatile tool for mass spectrometry quantification** *Proteomics* **11**:3572–3577

56. Vannini A, Ringel R, Kusser AG, Berninghausen O, Kassavetis GA, Cramer P (2010) **Molecular basis of RNA polymerase III transcription repression by Maf1** *Cell* **143**

57. Wahlgren M, Goel S, Akhouri RR (2017) **Variant surface antigens of Plasmodium falciparum and their roles in severe malaria** *Nat Rev Microbiol*

58. Wullschleger S, Loewith R, Hall MN (2006) **TOR Signaling in Growth and Metabolism** *Cell* **124**:471–484

59. Zhang M, Wang C, Otto TD, Oberstaller J, Liao X, Adapa U SR, IF C K B, M B D M, et al (2018) **Uncovering the essential genes of the human malaria parasite Plasmodium falciparum by saturation mutagenesis** *Science*

60. Zhang Q *et al.* (2014) **Exonuclease-mediated degradation of nascent RNA silences genes linked to severe malaria** *Nature* **513**:431–435

61. Zhang X, Deitsch KW (2022) **The mystery of persistent, asymptomatic Plasmodium falciparum infections** *Current Opinion in Microbiology* **70**

Article and author information

Gretchen Diffendall
Institut Pasteur, 1Universite Paris Cité, INSERM U1201, CNRS EMR9195, Paris, France, Sorbonne Université Ecole doctorale Complexité du Vivant ED515, Paris, France
ORCID iD: 0000-0002-0783-517X

Aurélie Claës
Institut Pasteur, 1Universite Paris Cité, INSERM U1201, CNRS EMR9195, Paris, France

Anna Barcons-Simon
Institut Pasteur, 1Universite Paris Cité, INSERM U1201, CNRS EMR9195, Paris, France, Sorbonne Université Ecole doctorale Complexité du Vivant ED515, Paris, France, Biomedical Center, Division of Physiological Chemistry, Faculty of Medicine, Ludwig-Maximilians- Universität München, Munich 82152, Germany

Prince Nyarko
Laboratory of Pathogen–Host Interaction (LPHI), CNRS, University of Montpellier, France

Florent Dingli
Institut Curie, PSL Research University, Centre de Recherche, CurieCoreTech Mass Spectrometry Proteomics, Paris, France
ORCID iD: 0000-0002-7715-2446

Miguel Santos
Instituto de Medicina Molecular João Lobo Antunes, Faculdade de Medicina da Universidade de Lisboa, Lisboa, Portugal

Damarys Loew
Institut Curie, PSL Research University, Centre de Recherche, CurieCoreTech Mass Spectrometry Proteomics, Paris, France
ORCID iD: 0000-0002-9111-8842

Antoine Claessens
Laboratory of Pathogen–Host Interaction (LPHI), CNRS, University of Montpellier, France, LPHI, MIVEGEC, CNRS, INSERM, University of Montpellier, France
ORCID iD: 0000-0002-4277-0914

Artur Scherf
Institut Pasteur, 1Universite Paris Cité, INSERM U1201, CNRS EMR9195, Paris, France
For correspondence: artur.scherf@pasteur.fr
ORCID iD: 0000-0003-2411-3328

Copyright

Editors

Reviewing Editor
Olivier Silvie
Sorbonne Université, UPMC Univ Paris 06, INSERM, CNRS, Paris, France

Senior Editor
Dominique Soldati-Favre
University of Geneva, Geneva, Switzerland

Reviewer #1 (Public Review):

Summary:

Asymptomatic malaria infections are frequent during the dry season and have been associated with lower cytoadherence of P. falciparum parasites and lower expression of variant surface antigens. The mechanisms underlying parasite adaptation during the low transmission season remain poorly understood. The authors previously established that members of the non-coding RNA RUF6 gene family, transcribed by RNA pol III, are required for expression of the main variant surface antigens in P. falciparum, PfEMP1, which drive parasite cytoadherence and pathogenicity. In this study, the authors investigated the contribution of RNA pol III transcription in the regulation of PfEMP1 expression in different clinical states, either symptomatic malaria cases during the wet season or asymptomatic infections during the dry season.

By reanalyzing RNAseq data from a previous study in Mali, complemented with RT-qPCR on new samples collected in The Gambia, the authors first report the down-regulation of RNA pol III genes (tRNAs, RUF6) in P. falciparum isolates collected from asymptomatic individuals during the dry season, as compared to isolates from symptomatic (wet season) individuals. They also confirm the down-regulation of var (DBLalpha) gene expression in asymptomatic infection as compared to symptomatic malaria. Plasma analysis in the two groups in the Gambian study reveals higher Magnesium levels in dry season as compared to wet season samples, pointing at a possible role of external factors. The authors tested the effect of MgCl2 supplementation on cultured parasites, as well as three other stimuli (temperature, low glucose, Ile deprivation), and show that Ile deprivation and MgCl2 both induce down-regulation of RNA pol III transcription but not pol I or pol II (except the active var gene). Using RNAseq, they show that MgCl2 supplementation predominantly inhibits RNA pol III-transcribed genes, including the entire RUF6 family. Conditional depletion of Maf1 leads to the up-regulation of RNA pol III gene transcription, confirming that Maf1 is a RNA pol III inhibitor in P. falciparum, as described in other organisms. Quantitative mass spectrometry shows that Maf1 interacts with RNA pol III complex in the nucleus, and with distinct proteins including two phosphatases in the cytoplasm. Using the Maf1 cKD parasites, the authors document that down-regulation of RNA pol III by MgCl2 is dependent on Maf1. Finally, they show that MgCl2 results in decreased cytoadherence of infected erythrocytes, associated with reduced PfEMP1 expression.

Strengths:

-The work is very well performed and presented.
-The study uncovers a novel regulatory mechanism relying on RNA pol III-dependent regulation of variant surface antigens in response to external signals, which could contribute to parasite adaptation during the low transmission season.
-Potential regulators of Maf1 were identified by mass spectrometry, including phosphatases, paving the way for future mechanistic studies.

Weaknesses:

-The signaling pathway upstream of Maf1 remains unknown. In eukaryotes, Maf1 is a negative regulator of RNA pol III and is regulated by external signals via the TORC pathway. Since TORC components are absent in the apicomplexan lineage, one central question that remains open is how Maf1 is regulated in P. falciparum. Magnesium is probably not the sole stimulus involved, as suggested by the observation that Ile deprivation also down-regulates RNA pol III activity.
-The study does not address why MgCl2 levels vary depending on the clinical state. It is unclear whether plasma magnesium is increased during asymptomatic malaria or decreased during symptomatic infection, as the study does not include control groups with non-infected individuals. Along the same line, MgCl2 supplementation in parasite cultures was done at 3mM, which is higher than the highest concentrations observed in clinical samples.
-Although the study provides biochemical evidence of Maf1 accumulation in the parasite nuclear fraction upon magnesium addition, this is not fully supported by the immunofluorescence experiments.

https://doi.org/10.7554/eLife.95879.2.sa2

Reviewer #2 (Public Review):

The study by Diffendall et al. set out to establish a link between the activity of RNA polymerase III (Pol III) and its inhibitor Maf1 and the virulence of Plasmodium falciparum in vivo. Having previously found that knockdown of the ncRNA ruf6 gene family reduces var gene expression in vitro, they now present experimental evidence for the regulation of ruf6 and subsequently, var gene expression by Pol III using a commercially available inhibitor. They confirm their findings with samples from a previously published Gambian cohort study using asymptomatic dry season and mildly symptomatic wet season samples, showing that higher levels of Pol III-dependent transcripts and var transcripts as well as lower MgCl2 plasma concentrations are present in wet season samples. From this, they hypothesize that the external stimuli heat, reduced glucose and essential amino acid supply, and increased MgCl2 levels are sensed by the parasite through the only known Pol III inhibitor Maf1 and result in lower Pol III activity and fewer ruf6 transcripts, which in turn reduces var gene expression, leading to reduced cytoadherence and virulence of P. falciparum. In their in vitro experiments they focus on investigating higher MgCl2 levels and their impact on Pol III and Maf1 activity as well as var gene expression and parasites adherence to purified CD36, thereby successfully confirming their hypothesis for MgCl2. Nicely, MgCl2-induced down-regulation of Pol III activity was shown to be dependent on Maf1 using a knock-down cell line. Additionally, they show that the Maf1-KD cell line displays a slower growth rate with fewer merozoites per schizonts and Maf1 interacts with RNA pol III subunits and some kinases/phosphatases.

Comments on latest version:

It is understandable that the RNA samples from the Gambian cohort were limited, but for all in vitro analyses a larger panel of qPCR primers or RNAseq would have been feasible. I also understand the rationale for using the general var primer pair (DBLa) for field isolates, but since the authors were working with a clonal parasite line (3D7) in vitro, qPCR with specific 3D7/NF54 primer pairs or RNAseq, which would also allow inferences about ruf6 regulation of specific (neighboring?) var genes and other Pol III-regulated genes, would have been a far better option.

As far as I could see from the resubmitted manuscript, the authors did not correct the statistical analyses. For example, they continue to apply a t-test to fold-change values (which must be transformed to log2), many t-test based analyses rely on only 2-3 replicates (a non-parametric test would be more appropriate), they have not corrected for multiple testing, and it is unclear how the authors handle technical and biological replicates in their plots. Therefore, I still suspect that more appropriate statistical analyses might have an impact on the significance of their results.

I agree that CD36 binding is associated with mild malaria, but since the authors only make a link between Pol III and CD36 binding in vitro, I think it is an overstatement to claim something like "Our study reveals a regulatory mechanism in P. falciparum involving RNA Polymerase III, which plays a pivotal role in the parasite's virulence."

Finally, if the authors have checked all the relevant literature on MgCl2, it should be easy for them to give a brief explanation why they included only one study and ignored all the other contradictory results.

https://doi.org/10.7554/eLife.95879.2.sa1

Reviewer #3 (Public Review):

Summary:

This work describes a new pathway by which malaria parasites, P. falciparum, may regulate their growth and virulence (i.e. their expression of virulence-linked cytoadhesins). This is a topic of considerable interest in the field - does this important parasite sense factor(s) in its host bloodstream and regulate itself accordingly? Several fragments of evidence have come out on this topic in the past decade, showing, for example, reduced parasite growth under calorie restriction (in mice); parasite dormancy in response to amino acid starvation (in culture and in mice), and also reduced virulence in dry-season, low-parasitaemia infections in humans. The molecular mechanisms that may underlie this interesting biology remain only poorly understood.

Here, the authors show that dry-season P. falciparum parasites have reduced expression of Pol3-transcribed tRNAs and ncRNAs that positively regulate virulence gene expression. They link the level of Pol3 activity to PfMaf1, a remnant of the largely-absent nutrient-sensing TOR pathway in this parasite. They propose that in the dry season, human hosts may be calorie-restricted, leading to Maf1 moving to the nucleus and suppressing Pol3, thus downregulated growth and virulence of parasites. The evidence is intriguing and the idea is conceptually elegant.

Strengths:

The use of dry/wet-season field samples from The Gambia is a strength, showing potential real-world relevance. The generation of an inducible knockdown of Maf1 in lab-cultured parasites is also a strength, allowing this pathway to be studied somewhat in isolation.

Weaknesses:

(1) The signals upstream of Maf1 remain rather a black box. 4 are tested - heatshock and low-glucose, which seem to suppress ALL transcription; low-Isoleucine and high magnesium, which suppress Pol3. Therefore the authors use Mg supplementation throughout as a 'starvation type' stimulus. They do not discuss why they didn't use amino acid limitation, which could be more easily rationalised physiologically. It may for experimental simplicity (no need for dropout media) but this should be discussed, and ideally sample experiments with low-IsoLeu should be done too, to see if the responses (e.g. cytoadhesion) are all the same.

(2) The proteomics, conducted to seek partners of Maf1, is probably the weakest part. From Fig S4 it is clear that the proteins highlighted in the text are highly selected (as ones that might be relevant, e.g. phosphatases), but many others are more enriched. It would be good to see a) the top hits from the whole list provided as a short table within the main proteomics figure, along with the GO terms that actually came top in enrichment; b) the whole list provided as a supp. spreadsheet for easy re-analysis, rather than a PDF which cannot be easily re-used.

(3) Fig 3 shows the Maf1-low line has very poor growth after only 5 days but it is stated that no dead parasites are seen even after 8 cycles and the merozoites number is down only ~18 to 15... is this too small to account for such poor growth (~5-fold reduced in a single cycle, day 3-5)? It would additionally be interesting to see a cell-cycle length assessment and invasion assay, to see of Maf1-low parasite have further defects in growth.

Other weaknesses, which are more restricted but were not addressed in revision, are highlighted below:

Fig S1B - The downregulation of RNAPol3 transcripts caused by a commercial Pol3 inhibitor is pretty weak - mostly non-significant. The authors might comment on why they think this is, when interfering with PfMaf1 evidently has a greater effect.

Fig 2D: the legend states ' Expressed transcripts from three replicates between control and addition of MgCl2 that are significantly up-regulated are highlighted in red while significantly down-regulated RNA Pol III genes are highlighted in blue (FDR corrected p-value of <0.05) and a FC {greater than or equal to}{plus minus} 1.95) with examples listed as text'. This isn't very clear. The authors could clarify whether they took ALL (Pol3 or not) upregulated genes to show in red, but only putative Pol3-regulated genes to show in blue? If so, why? Or did they take all significantly downregulated genes, and found they were all annotated as pol3 transcribed? (I cannot see any dots that are not blue. If there are some, a clearer figure is needed?)

Line 227: 'PfMaf1 levels were shown to decrease by approximately 57% in total extracts after one cycle' - the provenance of this very precise percentage isn't clear (it does not appear on the figure). Is it densitometry of a western blot? And if so, is it an average of the 3 replicates that are stated in the legend (but not shown), or from the single example blot shown in Figure 3?

Fig 4A: the western blot, as shown, lacks controls, both for loading and for completeness of cyto/nuclear fractionation. To avoid confusion, these should be shown in the main figure, as is standard in the field, rather than separately in a supp figure. Ideally, 3 repeats should be done, with densitiometry quantification.

https://doi.org/10.7554/eLife.95879.2.sa0

Author response:

The following is the authors' response to the original reviews.

Here we address the major points raised by the reviewers.

> ***Reviewer #1 (Public Review):***
>
> *Weaknesses:*
>
> - *The signaling pathway upstream of Maf1 remains unknown. In eukaryotes, Maf1 is a negative regulator of RNA pol III and is regulated by external signals via the TORC pathway. Since TORC components are absent in the apicomplexan lineage, one central question that remains open is how Maf1 is regulated in P. falciparum. Magnesium is probably not the sole stimulus involved, as suggested by the observation that Ile deprivation also down-regulates RNA pol III activity.*

We agree that there is still much to uncover relating to the PfMaf1 signaling pathway. While we still do not know each component, we have been able to link external factors (of course not limited to only magnesium) to the increased nuclear occupancy of PfMaf1. Other protein interactors that potentially regulate PfMaf1, while not confirmed, have been identified in plasma sample as candidates for future experiments to validate their potential involvement of RNA Pol III inhibition.

> - *The study does not address why MgCl2 levels vary depending on the clinical state. It is unclear whether plasma magnesium is increased during asymptomatic malaria or decreased during symptomatic infection, as the study does not include control groups with non-infected individuals. Along the same line, MgCl2 supplementation in parasite cultures was done at 3mM, which is higher than the highest concentrations observed in clinical samples.*

This reviewer raised a valid point. The plasma magnesium levels for the wet symptomatic samples (averaging [0.79mM]) were within the normal range of a healthy individual (between [0.75-0.95mM]) while the dry asymptomatic levels were above the normal range (averaging [1.13mM]). Ideally, we would have liked to have control uninfected plasma samples from individuals from The Gambia. Unfortunately, field studies and human volunteer studies do not always have all the ideal controls that in vitro studies have. We recognize that [3mM] is higher than the normal range for magnesium levels, which is why we included a revised Supplementary Figure 3A. This figure shows that magnesium concentrations as low as [1mM] (similar to the levels found in dry asymptomatic samples) reduced the expression of RNA Pol III-transcribed genes.

> - *Although the study provides biochemical evidence of Maf1 accumulation in the parasite nuclear fraction upon magnesium addition, this is not fully supported by the immunofluorescence experiments.*

We agree that the resolution of IFA images does not allow to support the WB data. We believe that the importance of the IFA Supplementary Figure is to show that PfMaf1 clusters together in foci, which has not been previously reported.

> ***Public Reviews:***

Here we address the major points raised by the reviewers.

> ***Reviewer #1 (Public Review):***
>
> *Weaknesses:*
>
> - *The signaling pathway upstream of Maf1 remains unknown. In eukaryotes, Maf1 is a negative regulator of RNA pol III and is regulated by external signals via the TORC pathway. Since TORC components are absent in the apicomplexan lineage, one central question that remains open is how Maf1 is regulated in P. falciparum. Magnesium is probably not the sole stimulus involved, as suggested by the observation that Ile deprivation also down-regulates RNA pol III activity.*

We agree that there is still much to uncover relating to the PfMaf1 signaling pathway. While we still do not know each component, we have been able to link external factors (of course not limited to only magnesium) to the increased nuclear occupancy of PfMaf1. Other protein interactors that potentially regulate PfMaf1, while not confirmed, have been identified in plasma sample as candidates for future experiments to validate their potential involvement of RNA Pol III inhibition.

> - *The study does not address why MgCl2 levels vary depending on the clinical state. It is unclear whether plasma magnesium is increased during asymptomatic malaria or decreased during symptomatic infection, as the study does not include control groups with non-infected individuals. Along the same line, MgCl2 supplementation in parasite cultures was done at 3mM, which is higher than the highest concentrations observed in clinical samples.*

This reviewer raised a valid point. The plasma magnesium levels for the wet symptomatic samples (averaging [0.79mM]) were within the normal range of a healthy individual (between [0.75-0.95mM]) while the dry asymptomatic levels were above the normal range (averaging [1.13mM]). Ideally, we would have liked to have control uninfected plasma samples from individuals from The Gambia. Unfortunately, field studies and human volunteer studies do not always have all the ideal controls that in vitro studies have. We recognize that [3mM] is higher than the normal range for magnesium levels, which is why we included a revised Supplementary Figure 3A. This figure shows that magnesium concentrations as low as [1mM] (similar to the levels found in dry asymptomatic samples) reduced the expression of RNA Pol III-transcribed genes.

> - *Although the study provides biochemical evidence of Maf1 accumulation in the parasite nuclear fraction upon magnesium addition, this is not fully supported by the immunofluorescence experiments.*

We agree that the resolution of IFA images does not allow to support the WB data. We believe that the importance of the IFA Supplementary Figure is to show that PfMaf1 clusters together in foci, which has not been previously reported.

> ***Reviewer #2 (Public Review):***
>
> *Weaknesses:*

> *However, most analyses are rather preliminary as only very few (3-5) candidate genes are analyzed by qPCR instead of carrying out comprehensive analyses with a large qPCR panel or RNA-seq experiments with GO term analyses. Data presentation lacks clarity, the number of biological replicates is rather low and the statistical analyses need to be largely revised. Although the in vivo data from wet (mildly symptomatic) and dry (asymptomatic) season parasites with different expression levels of Pol III-regulated genes, var genes, and MgCl2 are interesting, the link between the in vitro data and the in vivo virulence of P. falciparum, which is made in many sections of the manuscript, should be toned down. Especially since (i) the only endothelial receptor studied is CD36, which is associated with parasite binding during mild malaria, and (ii) several studies provide contradictory data on MgCl2 levels during malaria and in different disease states, which is not further discussed, but the authors mainly focused on this external stimulus in their experiments.*

We agree that, ideally, we would have liked to do full RNA-seq on The Gambia samples. However, that was out of the scope of this project. The RNA samples were limited which is why we did not use more primers. We believe that an appropriate number of replicates was done for the experiments. The wet symptomatic samples from this study were from mildly symptomatic individuals, as stated in the manuscript. Therefore, CD36 was a relevant receptor to use for our studies.

We agree that the published studies about magnesium levels in infected individuals are not always consistent. What these studies do not consider is the time of year, whether the infection occurred during the dry or wet season. These studies were also done in different regions of the world using different technologies. For this reason, we only highlight the observed difference observed in our field study data from The Gambia.

> ***Reviewer #3 (Public Review):***
>
> *Weaknesses:*
>
> *(1) The signals upstream of Maf1 remain rather a black box. 4 are tested - heat shock and low-glucose, which seem to suppress ALL transcription; low-Isoleucine and high magnesium, which suppress Pol3. Therefore the authors use Mg supplementation throughout as a 'starvation type' stimulus. They do not discuss why they didn't use amino acid limitation, which could be more easily rationalised physiologically. It may be for experimental simplicity (no need for dropout media) but this should be discussed, and ideally, sample experiments with low-IsoLeu should be done too, to see if the responses (e.g. cytoadhesion) are all the same.*

We agree that deprivation of isoleucine would have been another experimental assay for our study, but it also would not have been as novel as magnesium. While understanding the exact mechanism or involvement of magnesium as a stress condition was not the scope of this manuscript, we believe that our data will be valuable into demonstrating that external stimuli act on P. falciparum virulence gene expression via RNA Pol III inhibition. Since we also had plasma level data for magnesium, and not isoleucine, we believed it made for a better external factor to use for our in vitro studies.

> *(2) The proteomics, conducted to seek partners of Maf1, is probably the weakest part. From Figure S3: the proteins highlighted in the text are clearly highly selected (as ones that might be relevant, e.g. phosphatases), but many others are more enriched. It would be good to see the whole list, and which GO terms actually came top in enrichment.*

We apologize if the reviewer did not see the attached supplementary Co-IP MS data. The file includes all proteins found in each sample as well as GO term analysis. For the purpose of this work, we highlight proteins potentially involved in the canonical role of Maf1 that have been shown in model organisms to reversibly inhibit RNA Pol III (phosphatases, RNA Pol III subunits).

> *(3) Figure 3 shows the Maf1-low line has very poor growth after only 5 days but it is stated that no dead parasites are seen even after 8 cycles and the merozoites number is down only ~18 to 15... is this too small to account for such poor growth (~5-fold reduced in a single cycle, day 3-5)? It would additionally be interesting to see a cell-cycle length assessment and invasion assay, to see if Maf1-low parasites have further defects in growth.*

We agree with the reviewer that the observed reduced merozoite numbers may not the only cause of the reduced growth rate. Other factors in the PfMaf1 knock-down line may contribute to the observed poor growth.